



ECONOMIC RESEARCH
FEDERAL RESERVE BANK OF ST. LOUIS
WORKING PAPER SERIES

The Dual Beveridge Curve

Authors	Anton Cheremukhin, and Paulina Restrepo-Echavarria
Working Paper Number	2022-021F
Revision Date	September 2025
Citable Link	https://doi.org/10.20955/wp.2022.021
Suggested Citation	Cheremukhin, A., Restrepo-Echavarria, P., 2025; The Dual Beveridge Curve, Federal Reserve Bank of St. Louis Working Paper 2022-021. URL https://doi.org/10.20955/wp.2022.021

Federal Reserve Bank of St. Louis, Research Division, P.O. Box 442, St. Louis, MO 63166

The views expressed in this paper are those of the author(s) and do not necessarily reflect the views of the Federal Reserve System, the Board of Governors, or the regional Federal Reserve Banks. Federal Reserve Bank of St. Louis Working Papers are preliminary materials circulated to stimulate discussion and critical comment.

The Dual Beveridge Curve

Anton Cheremukhin*

Paulina Restrepo-Echavarria†

September 29, 2025

Abstract

The U.S. Beveridge curve’s recent outward shift has puzzled economists. We argue that the key stylized fact requiring a new framework is the divergence between surging vacancies and stable hires from unemployment. We propose a dual-vacancy model that attributes this divergence to a rising share of “poaching” vacancies targeted at employed workers. The model’s core identification reveals a disconnect: the data force a conclusion that poaching vacancies account for most vacancy fluctuations, yet have a surprisingly small impact on actual job-to-job hiring. This mechanism is validated by a new empirical fact: across sectors, vacancy rates converged post-2010 while hiring strategies diverged—a puzzle our framework uniquely resolves. Estimating the model, we find that the share of poaching vacancies rose significantly, driven by an increased incentive to poach. Adjusting the Beveridge curve for this composition shift restores its historical stability.

Keywords: Beveridge Curve, Vacancies, Unemployment.

JEL Codes: J23, J63, J64, E52

*Federal Reserve Bank of Dallas, chertosha@gmail.com

†Federal Reserve Bank of St. Louis, paulinares@me.com

Declarations of interest: none. We thank Alessandro Barbarino, Serdar Birinci, Steven Davis, Marianna Kudlyak, Andreas Mueller, Nicolas Petrosky-Nadeau, Richard Rogerson, Ayşegül Şahin, Gianluca Violante, David Wiczer, Harald Uhlig, as well as participants of the seminar at the Dallas Fed, St. Louis Fed, and SED meetings in Barcelona for their insightful comments. The views expressed in this paper are those of the authors and do not necessarily reflect the views of the Reserve Banks of Dallas and St. Louis or the Federal Reserve System.

1 Introduction

The negatively sloped relationship between the number of unemployed individuals and the number of job openings over the business cycle, commonly known as the Beveridge curve, has served for decades as a central diagnostic tool in macroeconomics. First formalized in the postwar period, the curve provides a visual and quantitative representation of labor market tightness and matching efficiency, and has long been used by policymakers to assess the state of the labor market and gauge the distance to full employment.

In recent years, however, the behavior of the Beveridge curve has become increasingly difficult to interpret. As shown in Figure 1, the empirical curve has not only shifted outward but also changed slope in ways that depart significantly from historical patterns. Whereas previous recessions were characterized by movements along a relatively stable Beveridge curve with gradual shifts in intercept over time, the most recent episode—spanning the mid-2010s through the post-pandemic recovery—has seen abrupt and repeated changes in both slope and position. These changes have proven difficult to explain using standard narratives such as a sudden persistent decline in matching efficiency, which would need to be implausibly large to account for the data. This new behavior of the Beveridge curve presents an important puzzle.

The difficulty for standard models is not only empirical but also logical. If total vacancies rise sharply while hires from unemployment remain stable, then a single matching function can reconcile the two patterns only by assuming an implausibly large and persistent collapse in matching efficiency, a collapse in employed search effort, or an implausibly vertical Beveridge curve. None of these explanations are consistent with external evidence: efficiency is unlikely to fall precisely when recruitment technologies are improving, survey data show employed search remains robust, and empirical studies reject near-zero vacancy elasticities. The only coherent interpretation is that many of the additional vacancies are simply not relevant for unemployed workers.

In this paper, we formalize this idea by proposing a refinement of standard search-and-matching models: distinguishing between vacancies designed to hire unemployed workers and those intended to hire already-employed workers. While it is well understood that firms can choose to hire either from the pool of unemployed or by poaching workers already employed elsewhere, existing macroeconomic models typically treat all job vacancies as homogeneous. In contrast, we introduce a dual-vacancy model in which firms post two distinct types of vacancies: (i) those intended to be filled by unemployed individuals (non-poaching vacancies), and (ii) those targeting already-employed workers (poaching vacancies). These two vacancy types operate in segmented sub-markets with separate matching processes.

This distinction has direct implications for how we interpret movements in job vacancies. Vacancies targeting unemployed workers affect both the unemployment rate and the overall level of employment. In contrast, vacancies filled by poaching do not affect unemployment: they involve the reallocation of workers across jobs and may raise wages or improve match quality, but they do not alter employment aggregates. Therefore, in our framework, only non-poaching vacancies should be considered in the Beveridge curve relationship. Once we adjust the Beveridge curve to reflect this, the apparent breakdown in its behavior disappears.

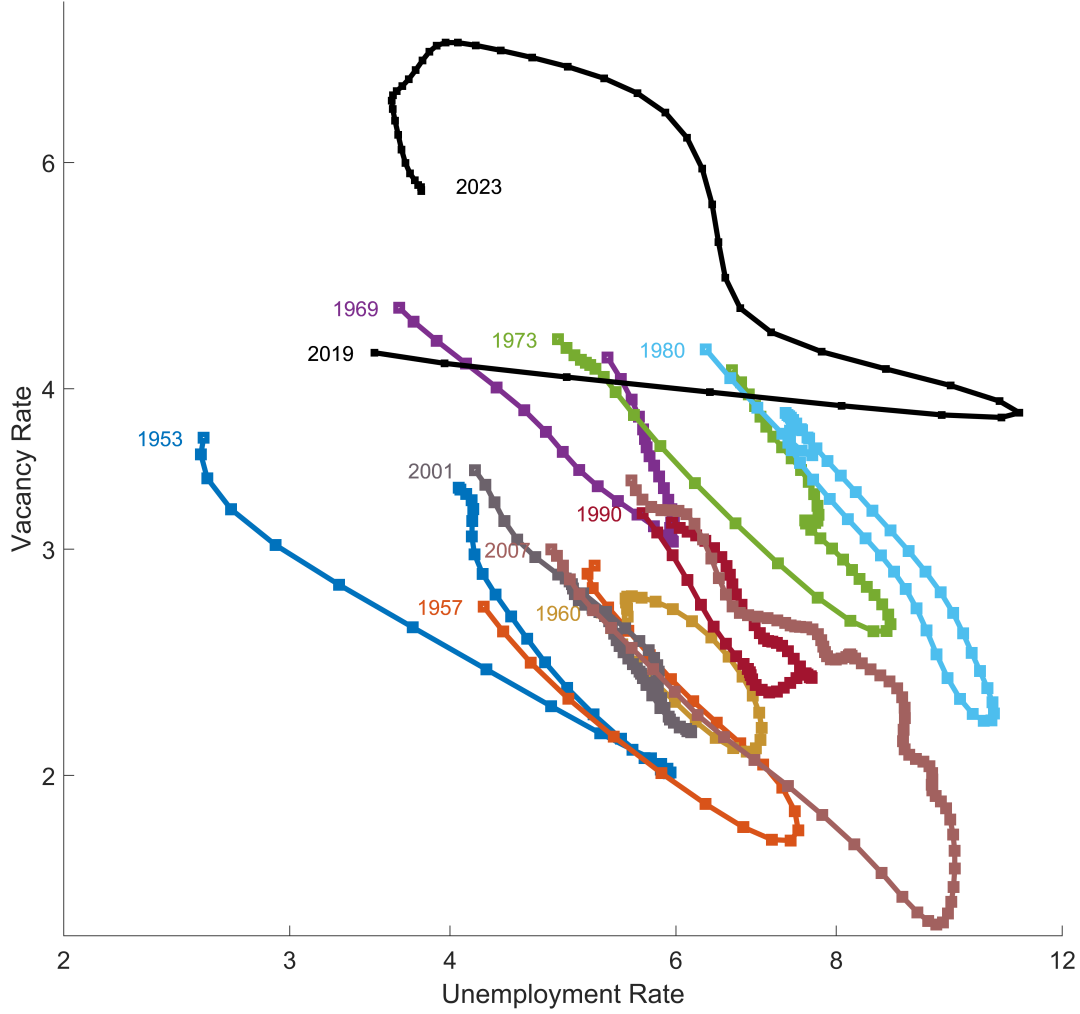


Figure 1: Beveridge Curves over Business Cycles.

Source: BLS. *Notes:* Henderson moving averages of the unemployment and vacancy rates are shown.

Our estimation reveals that this framework leads to an even starker conclusion about the nature of vacancies, dictated by two powerful tensions in the data. First, the divergence between the surging aggregate vacancy rate and the stable rate of hires from unemployment forces the model to attribute nearly all cyclical volatility and the entire post-2010 trend in vacancies to the poaching component. Consequently, non-poaching vacancies are found to be a much smaller, more stable series closely tied to unemployment dynamics.

Second, the model must then reconcile this highly volatile, trending series of poaching vacancies with the much more stable, observed rate of job-to-job transitions. The only way to do so is to conclude that the hiring of employed workers is almost completely insensitive to the number of poaching vacancies posted. Taken together, our findings suggest that the vast majority of measured vacancy fluctuations reflect a churning process for already-employed workers that has surprisingly little impact on actual hiring outcomes.

To precisely quantify these mechanisms, we estimate the dual-vacancy model using U.S. labor market data spanning 1978 to 2024. We draw on a wide array of data sources, including the Current Population

Survey (CPS), the Job Openings and Labor Turnover Survey (JOLTS), and reconstructed historical vacancy measures, as well as flow data from recent literature. This allows us to construct consistent time series of stocks and transitions among employment, unemployment, and nonparticipation.

Our estimation recovers the time path of each vacancy type and characterizes their dynamics. In our framework, hires are driven by a composite term that combines firms’ perceived profit-cost ratio of posting a vacancy and the underlying efficiency of the matching process. While these two components cannot be separately identified at business-cycle frequencies, we impose a minimal structure by assuming that the baseline matching efficiency follows a log-linear trend, without any abrupt breaks.¹ All higher-frequency fluctuations are therefore attributed to cyclical variations in the underlying drivers of vacancy creation.

Importantly, since the literature lacks consensus on how to best measure job flows, particularly EE rates and hires, we estimate the model under six plausible data configurations, spanning all combinations of CPS and JOLTS inputs and two alternative EE rate constructions. Our main findings hold robustly across all of them.

While direct data on vacancy intentions are not available, largely because equal opportunity employment laws prevent firms from stating explicit preferences for employed or unemployed applicants, we address this challenge by evaluating the extent to which our model fits the observed data better than a standard single-market model. We find that the dual-vacancy framework provides a significantly better fit to the data, particularly in its ability to jointly match the observed behavior of hires from unemployment and from employment. This improved fit reflects the fact that the responsiveness of these two flows to vacancy rates differs substantially — a feature the standard model cannot accommodate with a single elasticity.

In addition to showing that the dual-vacancy model fits the data better, we go further by explaining what drives the dynamics of the estimated vacancy split. A key contribution is showing how the evolution of each vacancy type is driven by an underlying, unobserved profit-cost ratio. Our decomposition reveals that the significant increase in poaching vacancies since the mid-2010s is primarily driven by a strong and persistent upward trend in their estimated profit-cost ratio, a pattern that predates the pandemic and persists across sectors.

Although our paper does not focus on policy analysis, our results have implications for how vacancy data should be interpreted in macroeconomic settings. When the share of poaching vacancies is large and rising, a decline in aggregate vacancies may translate into only a modest increase in unemployment. In such environments, aggregate vacancy measures may overstate the extent of labor market tightness that is relevant for the unemployed. This insight helps reconcile the recent coexistence of historically high vacancy rates and low unemployment with relatively mild changes in unemployment in response to shifts in labor demand. We return to these implications in the conclusion.

The model we estimate is statistical in nature, but closely aligned with canonical search-and-matching

¹Matching efficiency and vacancy profitability are not separately identified in our framework, as both affect hiring through the same structural channel. Our identifying assumption is that the long-run evolution of baseline matching efficiency is a trend process, a view supported by literature that attributes apparent efficiency shifts to factors like compositional mismatch rather than sharp changes in the matching technology itself (e.g., Şahin et al., 2014).

theory. It incorporates constant-returns-to-scale matching functions, free-entry conditions for vacancy creation, and a segmented structure for unemployed and employed job seekers. We include mechanisms to account for cross-matching between vacancy types, on-the-job search, and flows into employment from out of the labor force. Although our framework is not derived from micro-foundations or optimal choice behavior, its equilibrium structure is consistent with widely used theoretical models in the literature. We estimate the model using Bayesian methods, which offer a transparent and flexible framework for inference, particularly in models with latent variables like ours. The Bayesian approach facilitates joint estimation of trends and business-cycle fluctuations and ensures convergence in settings where multiple data sources and specifications are used.

Across six different data configurations and nine major sectors of the U.S. economy, we find robust evidence for our central claims. We show that the share of poaching vacancies increased substantially and persistently from the mid-2010s onward, driven by a structural shift in the incentives for firms to recruit already-employed workers. This shift in the composition of labor demand, rather than a decline in matching efficiency, is the key to understanding the recent turbulence in the Beveridge curve. Indeed, when we adjust the curve to include only non-poaching vacancies, its puzzling behavior disappears. Our analysis therefore provides a new framework for interpreting aggregate vacancy data, with important implications for policy and future research that we situate within the existing literature below.

Our paper contributes to three strands of the literature. First, we build on work analyzing the Beveridge curve, the inverse relationship between unemployment and vacancies, originally noted by Beveridge (1944) and formalized by Dow and Dicks-Mireaux (1958). This relationship has been studied extensively in both U.S. (e.g., Diamond and Şahin, 2014; Ahn and Crane, 2020) and international contexts (Hobijn and Şahin, 2012; Bonthuis et al., 2016), with recent shifts, especially outward movement and flattening, spurring renewed interest (Elsby, Michaels, and Ratner, 2015). We offer a new explanation for these shifts based on vacancy composition: once we exclude poaching vacancies, the Beveridge curve regains stability, narrowing the range of needed explanations.

These recent shifts have fueled both academic and policy debates. Lubik (2021) links them to reduced matching efficiency from sectoral change; Rodgers and Kassens (2022) cite altered incentives and demographics; others point to changes in job search technology. Most of these assume homogeneous vacancies. We instead highlight a rising share of vacancies targeting employed workers, altering the relationship between aggregate vacancies and unemployment. Our mechanism complements structural mismatch and friction-based explanations while implying that, during periods of tightening (e.g., Figura and Waller, 2022; Blanchard et al., 2022), unemployment may respond less to vacancy fluctuations due to shifts in labor demand composition.

Second, we contribute to the literature on matching functions. Traditional models (Pissarides, 1985, 2000; Mortensen and Pissarides, 1994) use a single function matching all job seekers to total vacancies. We instead estimate separate matching functions for vacancies targeting unemployed and employed workers, finding that this structure fits the data far better. A central result is that the elasticity of matching with respect to unemployment (α) is low — between 0.1 and 0.3 — well below standard estimates of 0.5–0.7 (Broersma and van Ours, 1999, Petrongolo and Pissarides, 2001). Our findings align with Gottfries and Stadin (2024),

who also find little evidence that higher unemployment increases vacancy filling speed, reinforcing our view that vacancy composition, not matching speed, drives Beveridge curve shifts.

Third, we contribute to the literature on labor market segmentation. Prior work has emphasized segmentation among workers: for example, Hall and Kudlyak (2020) and Ahn et al. (2022) identify heterogeneity in job seeker behavior. We extend segmentation to the firm side, estimating the composition of vacancies by intended hire type. While our aggregate, reduced-form framework is not explicitly micro-founded, its core premise aligns with the economic forces modeled in the targeted search literature (e.g. Cheremukhin and Restrepo-Echavarria, 2025), where heterogeneous firms can endogenously create segmented markets by targeting specific worker types. Our findings also complement the directed search framework of Menzio and Shi (2011) by providing empirical evidence for the aggregate importance of vacancy heterogeneity. Related work by Faberman et al (2022), and See, Birinci, and Wee (2024) documents systematic differences in job search behavior and transitions by employment status, supporting our model’s behavioral foundation.

Our findings also relate to recent work on vacancy heterogeneity. Qiu (2022) argues that many vacancies are unfilled or not seriously pursued, overstating labor demand. Along similar lines, we show that even filled vacancies differ in macro impact depending on their intended hire. Research on vacancy chains further supports our approach: Fujita and Nakajima (2016) show that poaching can trigger cascades of follow-up vacancies, while Elsby, Gottfries, Michaels, and Ratner (2025) provide direct evidence that many U.S. vacancies result from replacement hiring rather than net job creation. Mercan and Schoefer (2020) quantify how such chains shape aggregate vacancy dynamics. Together, these studies reinforce our finding that rising vacancies often reflect churn among employed workers, not increased hiring of the unemployed.

Adding to this literature, Afrouzi, Blanco, Drenik, and Hurst (2025) develop a model in which higher inflation encourages more job-to-job transitions, forcing firms to post additional vacancies to replace departing workers. This inflation-driven mechanism reinforces our central theme by showing how aggregate vacancies can rise due to market churn, without creating new opportunities for the unemployed.

In sum, our dual-vacancy framework offers a new lens on Beveridge curve dynamics and labor market tightness. It also cautions against interpreting aggregate vacancy data as a proxy for slack when poaching dominates vacancy growth. Beyond improving fit, our structure lays a foundation for future models incorporating vacancy types, search channels, and segmented labor market adjustment.

The paper is organized as follows. Section 2 presents the dual-vacancy model. Section 3 describes the data sources and measurement strategy. Section 4 presents our main empirical estimates and model parameters. Section 5 compares the fit of the dual-vacancy model to that of the standard single-vacancy framework. Section 6 analyzes the implications of our results for interpreting the Beveridge curve. Section 7 concludes with a discussion of broader implications and directions for future research.

2 Dual Beveridge Curve Model

Our statistical model builds on standard search-and-matching frameworks but does not explicitly model optimizing behavior. Instead, we specify matching functions, flow identities and equilibrium conditions rooted in canonical theory. These conditions will be familiar to readers from the search and matching literature. Rather than deriving each equation from first principles, we adopt a reduced-form approach that emphasizes identification and tractability while retaining a close structural link to the underlying theory.

The labor market in period t is characterized by a number of unemployed workers U_t searching for jobs, and a number of employed workers E_t , making together the labor force:

$$L_t = U_t + E_t. \quad (1)$$

Firms interested in employing workers post a number of vacancies V_t . A subset of employed workers, H_t , are interested in better job opportunities and actively search on the job. Some firms are interested in experienced workers and know that there is supply of such workers among the employed, so they design a subset of vacancy postings $V_{\epsilon,t}$ specifically to poach already employed workers. The rest of the vacancies $V_{u,t}$ (presumably low-level or entry positions) will consider and hire mostly unemployed workers. The total number of vacancies is a combination of these two types:

$$V_t = V_{u,t} + V_{\epsilon,t}. \quad (2)$$

The unemployed U_t search for non-poaching vacancies $V_{u,t}$ and get hired according to a standard constant-returns-to-scale matching function:

$$M_{u,t} = B_{u,t} U_t^\alpha V_{u,t}^{1-\alpha},$$

where $M_{u,t}$ is the number of hires from the unemployment pool, $\alpha \in [0, 1]$ is the matching elasticity, and $B_{u,t}$ characterizes the efficiency of the matching process.

A subset of employed workers H_t engage in on-the-job search and match with poaching vacancies $V_{\epsilon,t}$. The number of such matches is described by a second matching function:

$$M_{\epsilon,t} = B_{\epsilon,t} H_t^\beta V_{\epsilon,t}^{1-\beta},$$

where $M_{\epsilon,t}$ is the number of workers who quit their positions to join a new employer, $\beta \in [0, 1]$ is the matching elasticity, and $B_{\epsilon,t}$ is the efficiency of the matching process for already-employed workers.

We use a simplified version of a targeted search model (see Cheremukhin, Restrepo-Echavarria, and Tutino (2020)) as an inspiration to generalize our matching function specifications to the case where both types of workers sometimes confuse the two vacancy types and therefore apply to the wrong type of vacancy, so both types of vacancies run the risk of being filled by workers for which they were not originally designed. This confusion creates additional cross-matches, and their numbers should have the following forms: $M_{u,t}^+ = A_u U^\alpha V_{\epsilon,t}^{1-\alpha}$, and $M_{\epsilon,t}^+ = A_\epsilon H_t^\beta V_{u,t}^{1-\beta}$. These matches would be counted as unemployment-to-employment and employment-to-employment transitions respectively.

In addition, to accommodate the effect of substantial flows of workers between employment and out-of-the-labor-force states, we add a term capturing the potential matches of workers out of the labor force with total vacancies to produce additional flows into employment: $M_{u,t}^{++} = B_L N_t^\psi V_t^{1-\psi}$. To make the overall estimated expressions somewhat more flexible, we postulate the following general functional forms:

$$M_{u,t} = B_{u,t} U_t^\alpha V_{u,t}^{1-\alpha} \left[1 + A_u \left(\frac{V_{\epsilon,t}}{V_{u,t}} \right)^\gamma \right] + B_L N_t^\psi V_t^{1-\psi}, \quad (3)$$

$$M_{\epsilon,t} = B_{\epsilon,t} H_t^\beta V_{\epsilon,t}^{1-\beta} \left[1 + A_\epsilon \left(\frac{V_{u,t}}{V_{\epsilon,t}} \right)^\gamma \right], \quad (4)$$

where the mixing coefficients A_u and A_ϵ are the fractions of unemployed workers that are able to get a job with a firm that intended to poach and of employed workers that take up jobs intended for the unemployed. The elasticity γ adds flexibility by allowing the cross terms to reflect variations in either of the vacancy types. The parameter ψ captures the matching elasticity with respect to the number of civilians out of the labor force N_t and total vacancies V_t , and parameter B_L captures the matching efficiency.

The stock of employment increases when unemployed (or out of the labor force) workers find jobs, but declines when employed workers are laid off:

$$E_{t+1} = E_t (1 - s_t) + M_{u,t}, \quad (5)$$

where s_t is the layoff/separation rate. Note that matches created by employed workers and vacancies do not enter this equation. This is because when a person leaves a job and moves into a different job, the number of employed workers does not change.

We also need to make assumptions about the search effort of employed workers, H_t . In a study of search effort of workers searching on the job Faberman et al (2022) find that on average 78 percent of employed workers do not search at all, while the remaining 22 percent search even more effectively than the unemployed. While this study does not shed light on how this share varies over the business cycle, it stands to reason that it should vary with employment. As the baseline, we assume that there is the slow-moving bulk of employed workers, on average accounting for 78 percent of employment, that do not search. A simple proxy for this fraction would be a smoothed out trend of employment multiplied by 0.78. To compute a smoothed trend we HP-filter the employment series with parameter 10^6 , and denote it E_t^* . We assume that the rest of employed search at full strength, as much as the unemployed:

$$H_t = E_t - \xi_t E_t^*, \quad (6)$$

where ξ_t is the share of employed that do not search. We calibrate it to be 0.78 on average but let it vary over time and estimate it as an unknown shock.

To close the model, we need to add equations determining how many vacancies of each type are posted. The search and matching literature usually does this by assuming a free entry of vacancies, whereby vacancies

are added until their expected benefit equals their cost. As a result, the vacancy filling rate times the profit-cost ratio for each vacancy type equals one:

$$\frac{M_{u,t}}{V_{u,t}} y_t = 1, \quad (7)$$

$$\frac{M_{\epsilon,t}}{V_{\epsilon,t}} z_t = 1, \quad (8)$$

where y_t and z_t denote the profit-cost ratios for vacancies designed for the unemployed and poaching vacancies respectively.

We further simplify the model and notation by detrending by the labor force, for each variable X defining a lower case detrended analog $x_t = X_t/L_t$. This simplifies the model to the following 8-equation system:

$$\begin{aligned} (1) \quad m_t^u &= B_t^u u_t^\alpha v_{u,t}^{1-\alpha} \left(1 + A_u \left(\frac{v_{\epsilon,t}}{v_{u,t}} \right)^\gamma \right) + B_L n_t^\psi v_t^{1-\psi} \\ (2) \quad m_t^\epsilon &= B_t^\epsilon h_t^\beta v_{\epsilon,t}^{1-\beta} \left(1 + A_\epsilon \left(\frac{v_{u,t}}{v_{\epsilon,t}} \right)^\gamma \right) \\ (3) \quad v_{u,t} + v_{\epsilon,t} &= v_t \\ (4) \quad h_t &= e_t - \xi_t e_t^* \\ (5) \quad e_t + u_t &= 1 \\ (6) \quad e_{t+1} \delta_{l,t} &= e_t (1 - s_t) + m_t^u \\ (7) \quad v_{u,t} &= m_t^u y_t \\ (8) \quad v_{\epsilon,t} &= m_t^\epsilon z_t \end{aligned}$$

where $\delta_{l,t}$ is the growth rate of the labor force. The model is defined by a system of endogenous variables ($e_t, u_t, v_{u,t}, v_{\epsilon,t}, m_t^u, m_t^\epsilon, h_t, v_t$) that are driven by a set of exogenous shock processes ($y_t, z_t, s_t, \xi_t, \delta_{l,t}, e_t^*, n_t$) and two matching efficiency terms (B_t^u, B_t^ϵ).

A key aspect of our identification strategy concerns the treatment of shocks to matching efficiency. We assume that the baseline matching efficiencies, B_t^u and B_t^ϵ , evolve along deterministic log-linear trends. This approach is motivated by our argument that an abrupt, structural collapse in matching efficiency is implausible. However, we explicitly allow for higher-frequency, cyclical fluctuations in matching efficiency. Because such fluctuations are structurally indistinguishable from shocks to vacancy profitability, we do not model them as independent processes. Instead, any cyclical variation in matching efficiency is captured within our estimated composite shock series, y_t and z_t .

To estimate the model, we use nine observable time series, each measured with a white-noise error: the unemployment rate (u_t), the vacancy rate (v_t), hires from unemployment (m_t^u), hires from employment (m_t^ϵ), the separation rate (s_t), the employment-to-employment transition rate (ee_t), the labor force growth rate ($\delta_{l,t}$), the share of the population not in the labor force (n_t), and the trend component of the employment rate (e_t^*). For the EE rate, we consider two specifications based on how search effort is measured: hires as a share of total employment ($ee_t = \frac{m_t^\epsilon}{e_t}$, Variant A) and as a share of active searchers ($ee_t = \frac{m_t^\epsilon}{h_t}$, Variant B).

Finally, to account for the low-frequency movements in the data, we assume that the seven exogenous shock processes fluctuate around piece-wise linear time trends in an autoregressive manner. As detailed in Appendix A, we parameterize these trends, link them to the trends in the observable data, and use this structure to detrend all series before log-linearizing the model for estimation.

3 Data

Here we describe the data we use for our estimation. The first primary source of data is the Bureau of Labor Statistics, from which we use the Current Population Survey (CPS) and the Job Openings and Labor Turnover Survey (JOLTS). The CPS provides data on the Civilian Labor Force (1), composed of Employed (2) workers and Unemployed (3) workers, and the Civillians Not in the Labor Force (4), all four series for at least 16 year-olds, for the period from January 1978 to December 2024.

The CPS provides a Research dataset measuring flows of workers between the three states - Employment, Unemployment and Not-in-the-Labor-Force. We use headcounts measuring flows from Employment to Unemployment (EU flow, 5) and from Unemployment to Employment (UE flow, 6), for the period from February 1990 to December 2024.

The CPS dataset has been used by Fujita, Moscarini and Postel-Vinay (FMP, 2024), our second data source, to compute the rate at which workers transit between jobs (EE rate, 7), for the period from October 1994 to December 2024. We use their rate and multiply it by the number of Employed workers (2) to obtain a measure of employed workers that found a new job each month (EE flow).

The JOLTS provides monthly headcounts for total Hires (8), total Separations, containing Quits (9) and Layoffs (10), as well as total Job Openings (11), for the period from December 2000 to December 2024.

The CPS dataset has also been used by Ellieroth and Michaud (2024), our third data source, to measure transition rates from Employment to Unemployment (EU rate, 12) and Employment to Not-in-the-Labor-Force (EN, 13), and break each of these flows into voluntary separations (Quits,14, EUQ,15, ENQ,16) and involuntary separations (Layoffs, 17, EUL, 18, ENL, 19), for the period from January 1978 to December 2024. This dataset is notable because it infers from the CPS a series for Quits (14) which for the overlapping period is very similar to JOLTS data (9), and a series for Layoffs (17) which also for the overlapping period is very similar to JOLTS data (10). At the same time, the total EN flow (13) thus measured from the CPS is nearly indistinguishable from the EE rate (7), and both the EN and EU flows (12,13) are consistent with those reported by the CPS directly (5). The rates measured by Ellieroth and Michaud (EM, 2024) therefore bring together in a consistent way the CPS and JOLTS datasets, and extend both back in time to January 1978.

In addition, we use the methodology developed by Barnichon (2010) that extends the JOLTS measure of total job openings (11) back in time to 1951 using the Conference Board help-wanted index of online and newspaper advertising (20), our fourth data source.

To remove structural trends relating to the size of labor supply, we convert all the raw headcounts we

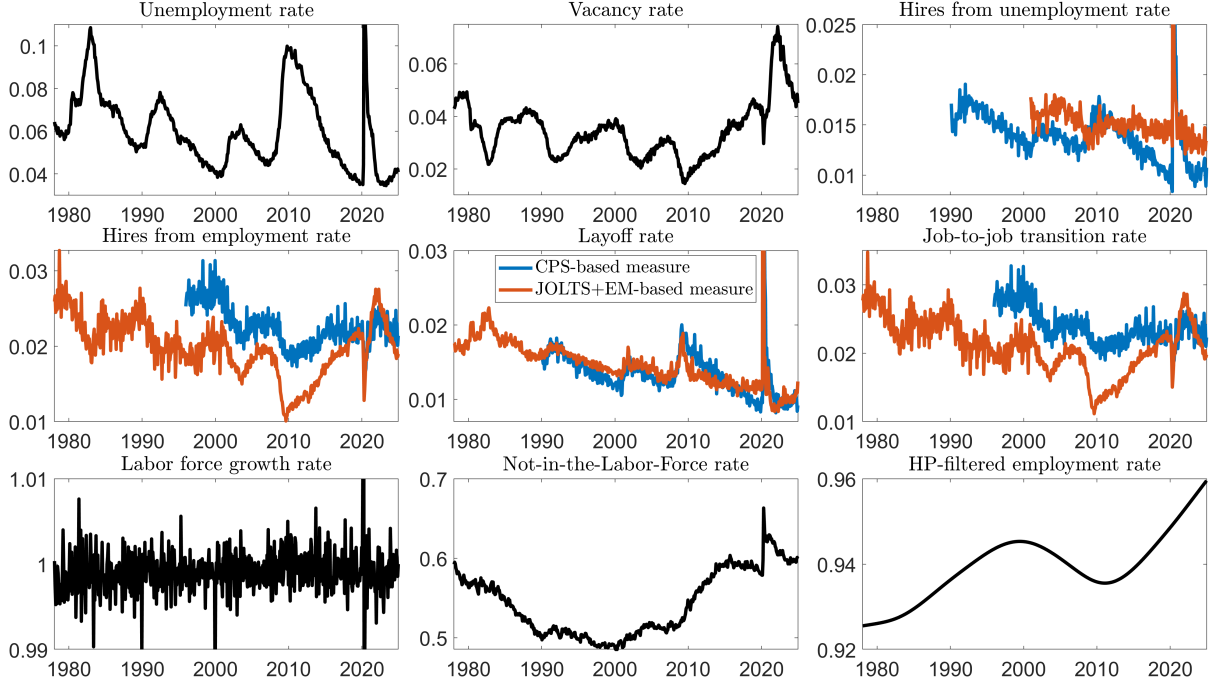


Figure 2: Data used in the Estimation.

Source: BLS, Fujita, Moscarini, Postel-Vinay (2024), Ellieroth, Michaud (2024), Barnichon (2010), Conference Board.

described earlier to rates relative to the labor force. This brings the measured series close to stationarity and in accordance with the assumptions of our model. As the measure of the unemployment rate u_t we take the number of unemployed (3) divided by the labor force (1). As the measure of the vacancy rate v_t we take the number of vacancies (11,20) divided by the labor force (1). As the measure of the exogenous variable $\delta_{l,t}$ we take the growth rate of the labor force (1). As the measure of not in the labor force n_t we take the number of not in the labor force (4) divided by the labor force (1). As the measure of HP-filtered employment e_t^* we take the number of employed (2) divided by the labor force (1) HP-filtered with parameter 10^6 .

For the remaining measures of (EU,UE,EE flows) we are left with more than one option. For the hires from unemployment flow m_t^u we have two options: 1) UE flow from the CPS (6) for 1990-2024, 2) Hires (8) minus Quits (9) from JOLTS for 2000-2024, — each in turn divided by the labor force (1) and in natural logs. For the hires from employment flow m_t^e we also have two options: 1) EE flow computed from the CPS as EE rate by FMP (7) multiplied by Employment (2) for 1995-2024, 2) Quits (9) from JOLTS extended using the series by EM (14) for 1978-2024, — each in turn divided by the labor force (1) and in natural logs. For the layoff/separation rate s_t we have two options as well: 1) EU flow computed from the CPS extended using the series by EM (12) for 1978-2024, 2) Layoffs (10) from JOLTS extended using the series by EM (17) for 1978-2024, — each in turn divided by Employment (2) and in natural logs. Finally, the EE rate ee_t that we use in the estimation is computed by dividing the EE flow described earlier by Employment (2), and taking natural logs. We consistently use the the same option for hires from employment flow and the EE rate. Each of the series and their options are shown in Figure 2 below.

We estimate the model under six configurations, combining three sets of hiring/separation data with two methods of interpreting employment-to-employment (EE) rates: A-variant uses hires divided by employment; B-variant uses hires divided by estimated on-the-job search effort. The three sets of hiring separation data include: 1) all series are sourced from CPS; 2) hires rates from the CPS, but Separation/Layoff rates from JOLTS; 3) all four series from JOLTS. We label the six estimation configurations CPS-A/B, Hybrid-A/B, and JOLTS-A/B, respectively. This multi-pronged estimation strategy ensures our findings are not artifacts of a particular data source or flow measurement method. It highlights the model’s ability to fit labor market dynamics robustly across all commonly used constructions.

4 Results

Identification: Linking Model and Data Before presenting our formal Bayesian estimation results, we begin with a detailed discussion of the identification logic that underpins our model. This logic clarifies why standard search-and-matching models fail to account for key labor market dynamics in the post-2010 U.S. economy and motivates our dual-vacancy framework as a necessary generalization. The estimation that follows can be viewed as a disciplined implementation of this data-driven logic.

The core puzzle, illustrated in Figure 2, lies in the divergence between total vacancies v_t and hires from unemployment m_t^u . While v_t exhibits a dramatic and sustained post-2010 upward trend documented across multiple sources, including JOLTS and alternative vacancy indices (e.g., the Help Wanted Online Index from Lightcast and the Indeed Hiring Lab; see also Mongey and Horwich, 2024), the hires rate from unemployment m_t^u and the job-finding rate m_t^u/u_t remain stable and show no comparable trend break.

Under a standard constant-returns-to-scale (CRS) matching framework, unemployed and employed job seekers search across a single vacancy pool, hires from unemployment satisfying: $m_t^u = B_t \cdot u_t \cdot \left(\frac{v_t}{u_t + h_t} \right)^{1-\alpha}$. To reconcile a surging v_t with stable m_t^u and u_t , one of four counterfactual conditions must hold:

1. *Collapse in Matching Efficiency (B_t):* Matching efficiency would need to decline sharply and persistently to offset the rise in v_t , a proposition inconsistent with the proliferation of efficiency-enhancing hiring technologies (e.g., online platforms, ATS software).
2. *Collapse in Employed Search Effort (h_t):* Employed search would have to fall substantially, boosting the relative share of unemployed matches. However, survey data from the NY Fed’s Survey of Consumer Expectations show that a stable and substantial share of employed workers continue to search on the job.
3. *Near-Zero Matching Elasticity ($\alpha \approx 1$):* Implies an implausibly vertical Beveridge curve, sharply at odds with the empirical literature.
4. *Vacancy Market Segmentation:* The standard matching function is misspecified. A growing share of aggregate vacancies are irrelevant for unemployed job seekers.

The implausibility of the first three conditions points to the fourth: segmentation in the vacancy market. Our dual-vacancy model formalizes this insight by positing separate matching functions for the unemployed and employed. Specifically, we estimate enhanced versions of $m_t^u = B_{u,t} \cdot u_t^\alpha \cdot v_{u,t}^{1-\alpha}$, $m_t^e = B_{e,t} \cdot h_t^\beta \cdot v_{e,t}^{1-\beta}$, where $v_{u,t}$ are vacancies targeting unemployed workers, and $v_{e,t} = v_t - v_{u,t}$ are poaching vacancies targeting employed workers.

Because m_t^u and u_t remain stable post-2010, $v_{u,t}$ must also be relatively stable. This pins down the non-poaching component of total vacancies. The remainder, $v_{e,t}$, absorbs the entire trend and excess volatility in v_t . The matching elasticity α is identified from the relative cyclical volatilities of m_t^u and u_t . Since hires are less volatile than unemployment, the model estimates a low α . In contrast, the poaching vacancy series $v_{e,t}$, inferred as the residual, is highly volatile and exhibits a strong post-2010 trend increase. Yet, the observed job-to-job flow series m_t^e remains relatively smooth. Reconciling an explosive input ($v_{e,t}$) with a stable output (m_t^e) requires the matching elasticity β to be close to 1.

In specifying the model, we have also assumed that matching efficiency follows a log-linear trend over time, without breaks. Any higher-frequency fluctuations in efficiency cannot be separately identified and are therefore subsumed into the estimated profit-cost ratios y_t and z_t . The assumption of a log-linear trend is consistent with our earlier argument that large trend breaks in efficiency are implausible, while still allowing the model to fully capture short-run variation in search effort and matching efficiency, lumped together with vacancy profitability through y_t and z_t .

Appendix B formalizes our identification strategy. The model is log-linearized and the mapping from observed to latent variables is inverted in closed form. Estimation then chooses parameters to maximize marginal data density, effectively minimizing the propagation of high-volatility inputs (v_t , u_t) into observed match flows. To avoid implausible volatility in m_t^u , the estimation pushes cross-market spillovers, governed by A_u and γ , toward zero, isolating the unemployed segment. Similarly, to mute the propagation from volatile $v_{e,t}$ to m_t^e , the estimation favors β close to 1.

In summary, identification flows from two central tensions: *stable m_t^u but surging v_t* necessitates a stable $v_{u,t}$ and implies that the upward trend is absorbed by poaching vacancies, *stable m_t^e but volatile $v_{e,t}$* necessitates near-unit β , shutting down the influence of $v_{e,t}$ on job-to-job flows. These tensions yield our main result: most fluctuations in aggregate vacancies reflect poaching activity, which has little bearing on actual job-to-job transitions and even less on the prospects of the unemployed. This mechanism explains the puzzling post-2010 shifts in the Beveridge curve without invoking implausible movements in matching efficiency or search effort.

Aggregate Estimation We now proceed to formally estimate the dual-vacancy model to quantify the mechanisms outlined above. Our primary goal is to recover the latent time series for non-poaching and poaching vacancies ($v_{u,t}$ and $v_{e,t}$) and to estimate the key structural parameters, particularly the matching elasticities α and β . To do this, we employ a Bayesian approach, which is well-suited for estimating models with unobserved state variables and allows for a transparent handling of parameter uncertainty. The Bayesian approach is particularly useful here because some parameters may not be fully identified, and the

likelihood surface can exhibit flat regions or multiple local maxima. By combining the likelihood with relatively uninformative priors, the method introduces additional curvature into the parameter space, improving convergence and aiding exploration of the posterior distribution.

We evaluate the posterior distribution using a Random Walk Metropolis (RWM) algorithm, as described in An and Schorfheide (2007). For each model variant, we run multiple chains initialized at the posterior mode, generating a total of 100,000 draws. We monitor convergence by checking that acceptance rates stay between 0.2 and 0.5 and that posterior means are stable across chains.

Our detrending methodology first identifies long-run trends in the data. We find that the separation rate and the unemployment rate have long-term downward trends, consistent with the literature on the secular decline in U.S. labor market dynamism (e.g., Molloy et al., 2016) and the natural rate of unemployment (e.g., Crump et al., 2019). Critically, we find that the estimated profit-cost ratio for poaching vacancies, z_t , exhibits a trend break around 2011, with a positive slope emerging thereafter. It is this upward trend in the profitability of poaching that generates the corresponding trends in aggregate vacancies, poaching vacancies, and hires from employment in our estimated model.

The estimated model also recovers the full time series for the exogenous shocks y_t and z_t , representing the composite profit-cost ratios, and the resulting split of job openings into poaching and non-poaching types. We report the average of these series across all six of our data specifications in Figure 3, along with 90-percent confidence intervals to reflect uncertainty from both data measurement and parameter estimation.

Two key observations emerge from Figure 3. First, the share of poaching vacancies increases significantly after the mid-2010s. This trend is closely associated in both timing and magnitude with the rising trend

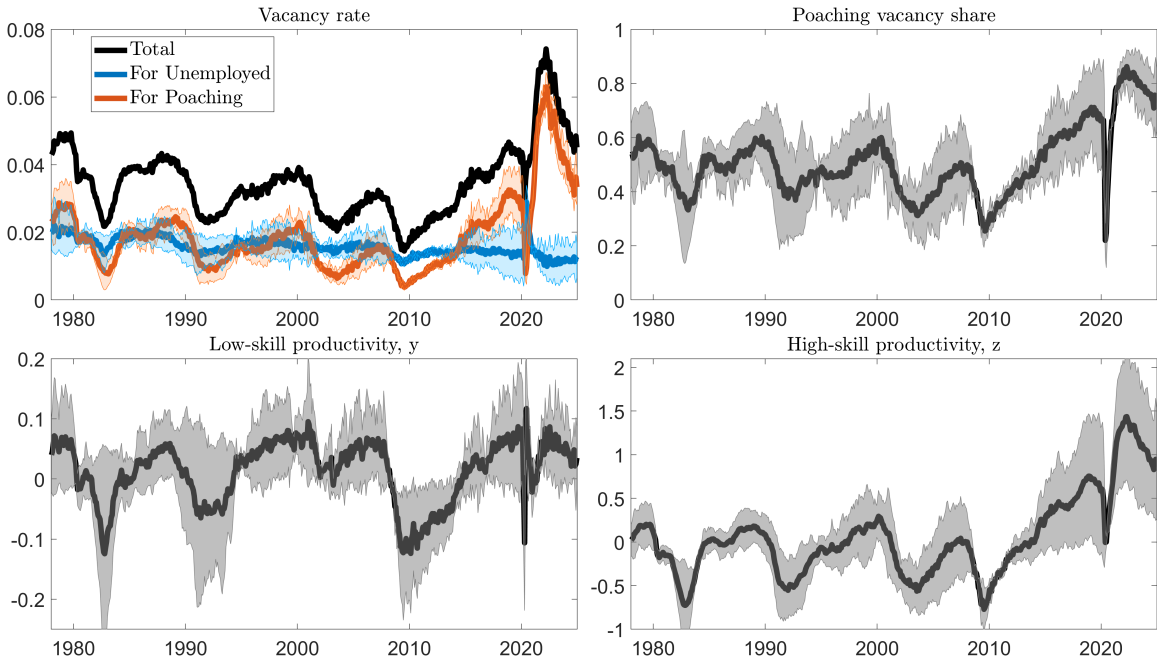


Figure 3: Estimated Shocks and Vacancy Split from 6 estimation setups.

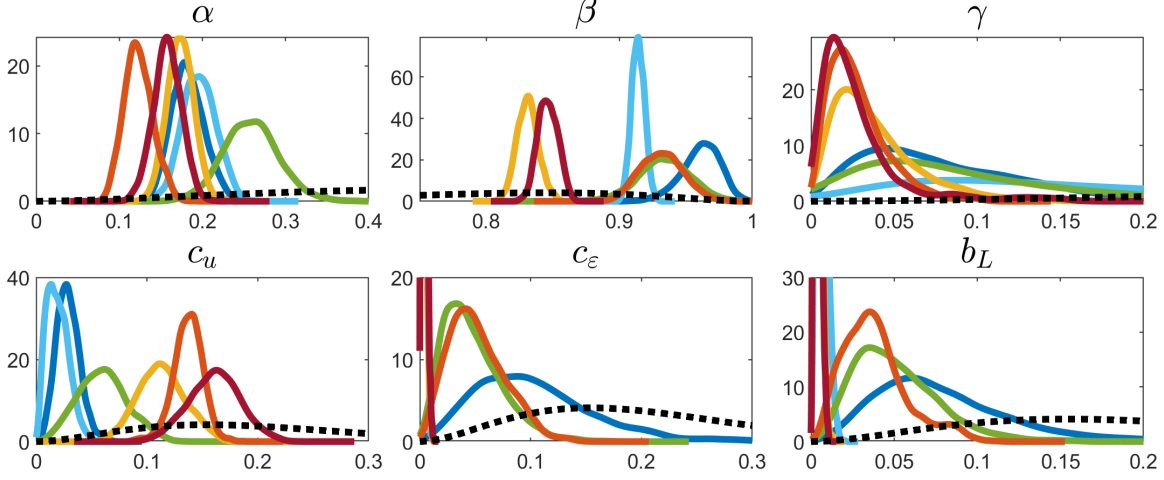


Figure 4: Prior and Posterior Estimates of Parameters for 6 estimation setups.

in the profit-cost ratio for poaching, z_t , suggesting the latter as the primary causal factor. Second, the business-cycle behavior of the two vacancy types diverges after 2015. While both types previously fell during recessions, in the 2020 recession poaching vacancies fell briefly and recovered, while non-poaching vacancies actually increased.

We now turn to the structural parameter estimates. Our estimated parameters using the CPS-A and JOLTS-A data specifications are shown in Tables 1 and 2. The estimates are very similar across specifications, a finding that holds more broadly across all six configurations as shown in Figure 4.

Confirming our identification logic, we estimate the matching elasticity for the unemployed, α , to be low, in the $[0.1-0.3]$ range, while the elasticity for the employed, β , is high, in the $[0.8-1]$ range. We also find that the cross-market spillover elasticity, γ , is close to zero, supporting the market segmentation hypothesis.

Table 1: Parameter estimates of the model in the CPS-A specification

Parameter	Prior			Posterior		
	mean	st.dev.	mode	mean	st. dev.	conf. int. [5-95]
α	0.5	0.2	0.157	0.166	0.014	[0.137, 0.194]
β	0.8	0.1	0.963	0.961	0.011	[0.939, 0.985]
γ	0.5	0.2	0.055	0.0692	0.030	[0.007, 0.128]
c_u	0.2	0.1	0.041	0.038	0.008	[0.022, 0.055]
c_ϵ	0.2	0.1	0.080	0.096	0.033	[0.026, 0.160]
b_L	0.2	0.1	0.098	0.089	0.029	[0.030, 0.147]

Notes: The priors for α , β , γ , c_u , c_ϵ were drawn from a beta distribution with support on the interval $[0, 1]$, prior for b_L was drawn from a gamma distribution with positive support.

Table 2: Parameter estimates of the model in the JOLTS-A specification

Parameter	Prior			Posterior		
	mean	st.dev.	mode	mean	st. dev.	conf. int. [5-95]
α	0.5	0.2	0.108	0.117	0.017	[0.090, 0.145]
β	0.8	0.1	0.929	0.921	0.015	[0.892, 0.947]
γ	0.5	0.2	0.017	0.025	0.013	[0.003, 0.046]
c_u	0.2	0.1	0.144	0.140	0.013	[0.117, 0.164]
c_ϵ	0.2	0.1	0.036	0.055	0.048	[0.009, 0.100]
b_L	0.2	0.1	0.033	0.053	0.015	[0.012, 0.096]

Notes: The priors for α , β , γ , c_u , c_ϵ , were drawn from a beta distribution with support on the interval $[0, 1]$, prior for b_L was drawn from a gamma distribution with positive support.

The log-linear parameters for cross-matching, c_u and c_ϵ ,² are likewise small, indicating that hires from the “wrong” vacancy type are infrequent. Finally, the share of net flows from out of the labor force is estimated to be modest, with a modal value for b_L around 3%.

Sectoral Estimation and External Validation To test the robustness and explore the heterogeneity of our aggregate findings, we next apply our estimation procedure to nine major sectors of the U.S. economy using JOLTS data from 2000–2024. This sectoral analysis serves two purposes. First, it allows us to verify that our core results—particularly the rising share of poaching vacancies—are a broad-based phenomenon and

²The parameters c_u and c_ϵ are the log-linear analogs of parameters A_u and A_ϵ in the full model, measuring the fractions of hires from employment and unemployment pools respectively that are formed using the wrong types of vacancies.

Table 3: Posterior (mode) estimates of parameters for sectors of the economy in the JOLTS-A specification

	α	β	γ	c_u	c_ϵ	b_L
Construction	0.066	0.990	0.014	0.109	0.057	0.047
Manufacturing	0.029	0.985	0.006	0.164	0.136	0.120
Transportation, Utilities	0.045	0.978	0.011	0.098	0.089	0.053
Wholesale Trade	0.081	0.967	0.016	0.090	0.060	0.040
Retail Trade	0.082	0.964	0.013	0.071	0.073	0.060
Business Services	0.037	0.979	0.013	0.141	0.081	0.052
Education, Health	0.019	0.944	0.007	0.124	0.144	0.079
Leisure	0.038	0.948	0.021	0.073	0.109	0.073
Government	0.003	0.975	0.010	0.106	0.134	0.035

Notes: The priors for α , β , γ , c_u , c_ϵ were drawn from a beta distribution with support on the interval $[0, 1]$, prior for b_L was drawn from a gamma distribution with positive support.

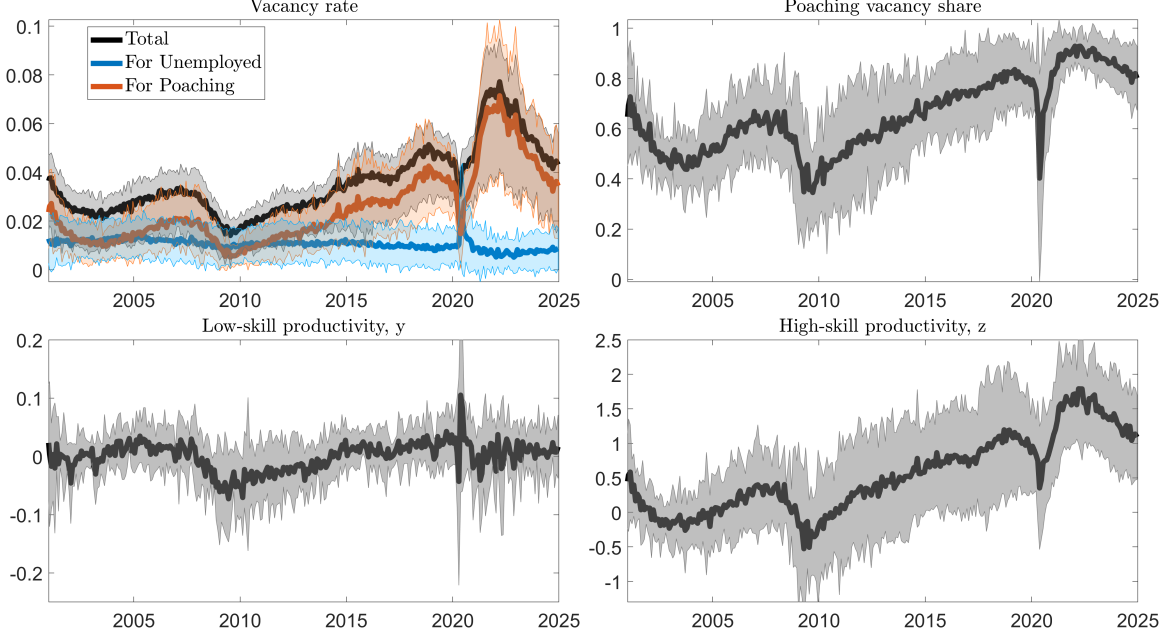


Figure 5: Estimated Shocks and Vacancy Split, across 9 sectors.

not driven by a single part of the economy. Second, and more importantly, it allows for a test of the model’s external validity. If our model is correctly identifying a meaningful economic distinction between poaching and non-poaching activity, then its internal findings should align with external, observable characteristics of sectoral labor markets.

The estimation results, reported in Table 3 and Figure 5, are broadly consistent with the aggregate findings across all nine sectors. We consistently estimate low values for α , high values for β , and near-zero spillovers (γ , c_u , c_e). In each case, the apparent upward trend in a sector’s total vacancies is driven by a rising trend in the estimated poaching component, which is in turn linked to the profitability shock z_t .

To provide a powerful, external validity test for our framework, we document a new stylized fact about the U.S. labor market and show that our dual-vacancy model is uniquely capable of explaining it. The puzzle lies in two seemingly contradictory cross-sectoral patterns that emerged between 2005 and 2019, a period spanning the pre- and post-Beveridge curve shift, as shown in Figure 6. First, we observe a strong convergence in sectoral vacancy rates (left panel). Sectors that began with lower vacancy rates in 2005 experienced significantly faster vacancy rate growth over the subsequent fourteen years. Second, and in stark contrast, we find a divergence in actual hiring strategies (right panel). Using data from the Census Bureau’s Job-to-Job Flows program, we measure a sector’s hiring strategy by its “J2J Share”—the share of total hires that come from other employers. Sectors that were already specialized in poaching in 2005 saw that share grow even larger by 2019, while sectors less reliant on poaching saw their share grow much less.

These two facts—converging vacancy effort alongside diverging hiring outcomes—present a deep puzzle for standard search-and-matching theory. In a conventional model with a single matching function and a typical vacancy elasticity, hiring outcomes are directly and elastically linked to vacancy posting. In such a

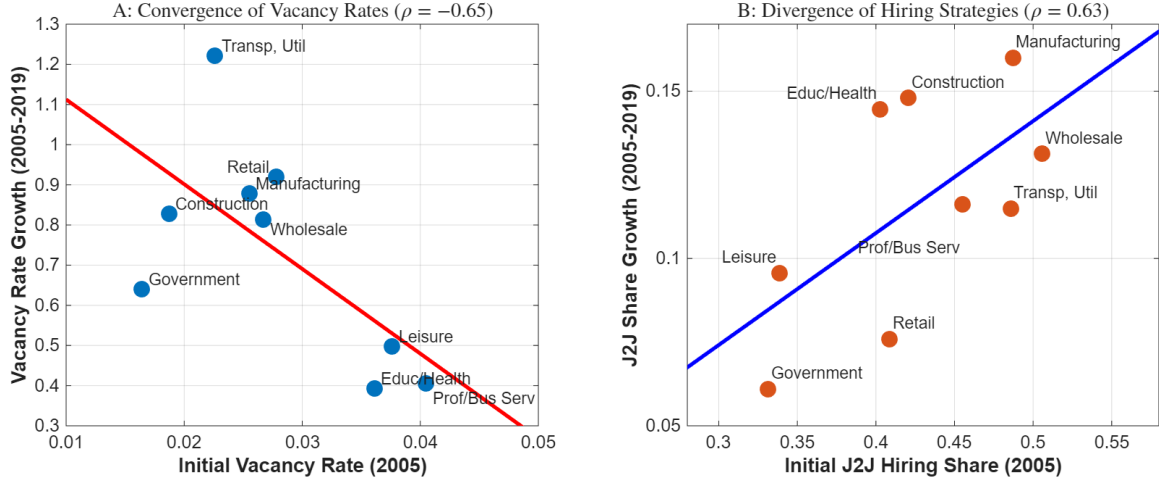


Figure 6: Convergence of vacancy rates, but divergence of hiring strategies.

world, a convergence in vacancy rates must lead to a convergence in hiring rates and, consequently, in hiring shares. A model with a stable, elastic link between vacancies and hires cannot simultaneously generate both patterns observed in the data. The contradiction suggests that this foundational assumption is flawed.

Our dual-vacancy model resolves this puzzle through its central estimate: the matching elasticity for employed workers, β , is close to unity. When $\beta \approx 1$, the number of actual job-to-job hires (m_t^e) becomes nearly disconnected from the number of poaching vacancies posted ($v_{e,t}$), and is instead governed by deeper, more slow-moving structural factors. This single finding explains how the two contradictory facts can coexist. The convergence in vacancy rates reflects a defensive “catch-up” in recruiting effort, as previously less-competitive sectors were forced to dramatically increase their vacancy posting to compete for talent. However, because $\beta \approx 1$, this surge in vacancy posting effort had a negligible impact on actual hiring outcomes. Only the sectors that were already structurally efficient at poaching could translate the new incentives into more job-to-job hires, leading them to specialize further and explaining the observed divergence in hiring strategies.

In conclusion, the documented divergence between hiring strategies and the convergence of vacancy rates provides strong external validation for our framework. It shows that the economy behaves as if the link between poaching vacancies and poaching hires is broken. Our model’s estimate of a near-unit β is not a statistical artifact, but the necessary economic mechanism to reconcile these stark empirical facts. Having established the core empirical results from our framework, we now provide formal evidence that this dual-vacancy structure is a necessary feature to explain the data by comparing its fit to a standard, single-market model.

5 Model Fit and Comparison with Standard Model

In our identification discussion in Section 4, we argued that a standard model with a single matching function cannot reconcile the divergent long-run trends in vacancies and hires. We now provide formal quantitative evidence that goes a step further: even after accounting for these trends, a standard model fails to match the fundamentally different business cycle dynamics of the two hiring margins. This failure to capture the cyclical properties of the data demonstrates the necessity of our dual-vacancy framework.

According to the standard model, a single constant-returns-to-scale matching function combines the total number of job seekers $U_t + H_t$ with the total number of vacancies V_t to produce the total number of matches $M_t^u + M_t^e$. To give the model its best chance of matching the data, we add extra flexibility to this overly restrictive model. We allow the proportion of total matches going to the unemployed to differ from their share of the search effort and estimate an additional parameter responsible for this split. Thus, our version of the traditional model consists of two equations with a single vacancy elasticity, $1 - \alpha$:

$$M_t^u = B_u U_t \left(\frac{V_t}{U_t + H_t} \right)^{1-\alpha}, \quad (9)$$

$$M_t^e = B_e H_t \left(\frac{V_t}{U_t + H_t} \right)^{1-\alpha}. \quad (10)$$

We replace the matching equations of our model with these alternative equations and estimate this traditional model using the same methods as our dual-vacancy model. This allows for a direct comparison of fit. The key restriction is that the traditional model has only one matching elasticity, α , and one aggregate series, V_t , to explain the dynamics of both hiring from unemployment and from employment. Meanwhile, the dual-vacancy model has two elasticities of the matching function, α and β , and recovers a hidden variable, the split of the vacancies.

The parameter estimates for the traditional model are presented in Table 4 and Figure 7. The estimates of the matching elasticity tend to be driven by the matching process for the unemployed and therefore give values for α in a range similar to the dual-vacancy model (see Tables 1 and 2). However, the inability of the model with a single matching function to explain the matching process for the employed leads to much poorer overall fit.

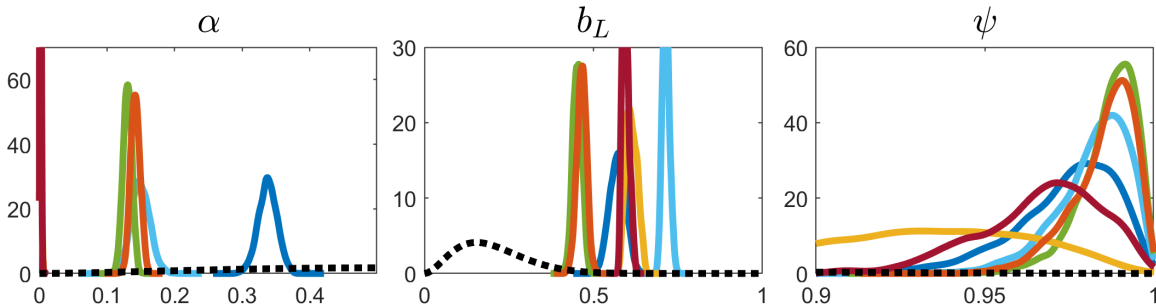


Figure 7: Estimated parameters of restricted model.

Table 4: Parameter estimates of the model with a single matching function

Parameter	Prior			Posterior		
	mean	st.dev.	mode	mean	st. dev.	conf. int. [5-95]
CPS-A						
α	0.5	0.2	0.32	0.32	0.015	[0.31, 0.35]
b_L	0.2	0.1	0.982	0.976	0.01	[0.956, 0.998]
ψ	0.5	0.2	0.59	0.59	0.03	[0.56, 0.63]
JOLTS-A						
α	0.5	0.2	0.141	0.145	0.005	[0.134, 0.155]
b_L	0.2	0.1	0.992	0.986	0.006	[0.974, 0.998]
ψ	0.5	0.2	0.46	0.46	0.01	[0.44, 0.49]

Notes: The priors for α , ψ were drawn from a beta distribution with support on the interval $[0, 1]$, prior for b_L was drawn from a gamma distribution with positive support.

Table 5: Comparison of model fit

Sector	Marginal Data Density		Bayes factor
	DVM	SMF	
CPS-A	9923	8972	exp(951)
CPS-B	9344	7940	exp(1404)
Hybrid-A	8985	7618	exp(1367)
Hybrid-B	9573	6086	exp(3486)
JOLTS-A	9427	7944	exp(1483)
JOLTS-B	9964	6406	exp(3559)

Notes: DVM stands for dual vacancy model, and SMF stands for single matching function model. The marginal data density was computed using Geweke’s (1999) modified harmonic mean method.

In Table 5 we present formal measures of model fit. The dual-vacancy model fits the data uniformly better based on marginal data density: in all six cases Bayes factors strongly favor the dual-vacancy model. The reason for this superior performance is now clear: the business cycle responsiveness of job-to-job flows to the vacancy rate is substantially different from that of hires from unemployment. A single matching function, constrained by a single elasticity, cannot simultaneously replicate these two different cyclical sensitivities. The dual-vacancy model, by allowing for two separate elasticities and, crucially, by having the ability to split vacancies into two components with different cyclical properties, does a much better job of fitting both margins.

The dual-vacancy model consistently outperforms the standard model in all configurations due to its ability to separately match poaching and non-poaching flows. This result provides strong statistical confirmation

of our initial identification logic. The divergence between the hiring margins is not just a feature of their long-run trends, but a fundamental property of their business cycle dynamics, which can only be explained by a model that allows for vacancy market segmentation. Having established that our dual-vacancy framework provides a statistically superior description of the data, we now turn to its most important economic implication: the reinterpretation of the Beveridge curve.

6 Dual Beveridge Curve

The key output of our estimation is the decomposition of total vacancies into a stable, non-poaching component relevant for the unemployed and a volatile, poaching component. This finding takes center stage in understanding the recent behavior of the Beveridge curve. Because only non-poaching vacancies match with unemployed workers and lead to net increases in employment, a properly specified Beveridge curve relationship should consider only this component and disregard poaching vacancies. The adjusted Beveridge curve for the whole economy is shown in the right panel of Figure 8, compared with the unadjusted (or classical) Beveridge curve in the left panel.

Figures 3 and 8 are illustrative of what happened in labor markets since the onset of the Covid pandemic. The first few months of the pandemic saw a decline in demand due to widespread social distancing, which increased unemployment and reduced poaching. In the next few months, mask and distancing mandates led to a separation shock where many more people were laid off than would be consistent with lower demand; so non-poaching vacancies increased, and a lot of people were hired back from unemployment very quickly. After the spike in hires from unemployment ended, stimulative fiscal and monetary policy increased purchasing power and created strong excess demand for goods. The excess demand prompted firms to expand, but this excess demand for workers could not be met by hiring from the unemployment pool. Together with supply chain bottlenecks, the excess demand for goods led to a surge in inflation; and excess demand for workers led to an increase in poaching, which then drove up nominal wage growth.

This interpretation provides us with two lessons. First, the (adjusted) Beveridge curve relationship between unemployed workers and non-poaching vacancies has not changed, at either the aggregate or sectoral level. In other words, the current puzzling behavior of the Beveridge curve disappears once we replace total vacancies with non-poaching vacancies. Second, abnormalities in the classical Beveridge curve are due to a disproportional expansion of poaching vacancies after 2010. Our estimation suggests that the underlying cause for this shift is the dramatic increase in the profit-cost ratio for poaching vacancies.

To better understand the shift, we can think of the steady-state version of our model and consider how it would be affected by a trend increase in the profit-cost ratio and the increase in the steady-state share of poaching vacancies. Equations of the model can be further simplified by substituting the matching functions

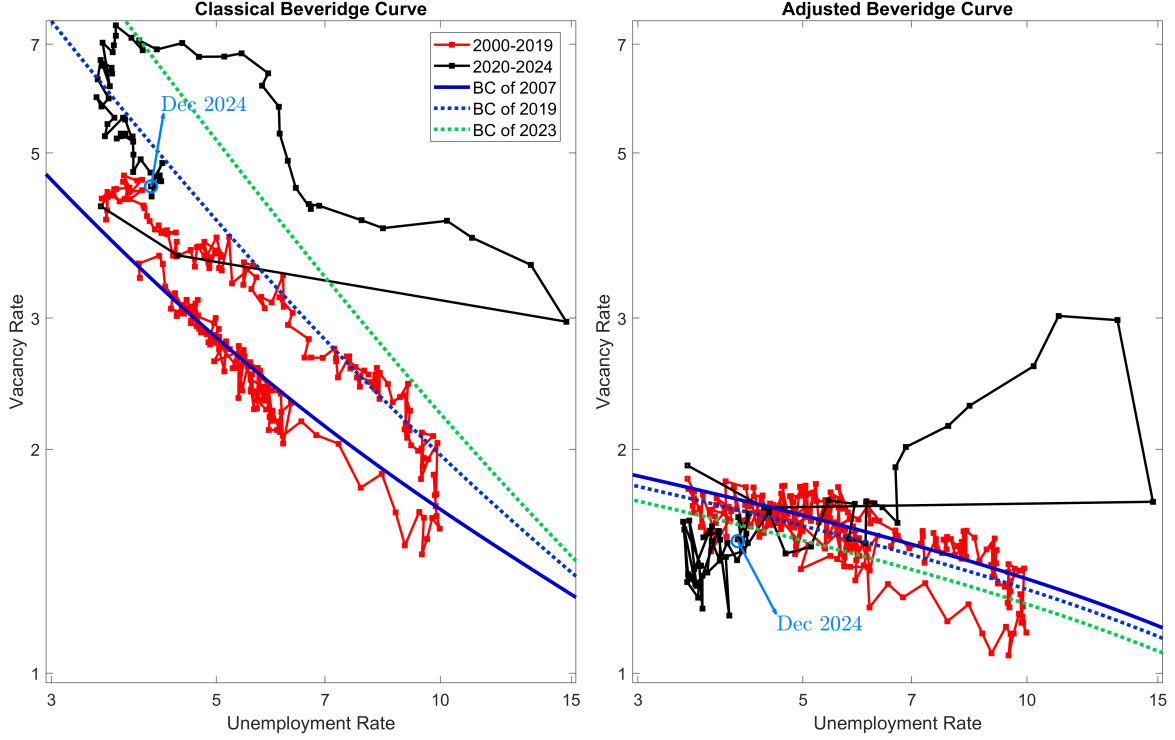


Figure 8: Classical and Adjusted Beveridge Curves

and the search effort of the employed to get:³

$$\begin{aligned} (1-u)s &= B_u u \left(\frac{v_u}{u} \right)^{1-\alpha}, \\ \left(\frac{v_u}{u} \right)^\alpha &= B_u y, \\ \left(\frac{v_\epsilon}{0.27-u} \right)^\beta &= B_\epsilon z. \end{aligned}$$

where we omitted the mixing matching terms for simplicity. Although these three equations have three endogenous variables u, v_u, v_ϵ , the first two equations could be solved separately with respect to u and v_u — whose relationship determines the adjusted Beveridge curve. Poaching vacancies are then determined by the third equation, driven by fluctuations in their profitability z and the unemployment rate. The solution to the model then looks as follows:

$$\begin{aligned} u &= \frac{1}{1 + \frac{B_u}{s} (B_u y)^{\frac{1}{\alpha}-1}}, \\ v_u &= u (B_u y)^{\frac{1}{\alpha}}, \\ v_\epsilon &= (0.27-u) (B_\epsilon z)^{\frac{1}{\beta}}. \end{aligned}$$

Log-linearizing the model with respect to u and v_u , we find that the slope of the adjusted Beveridge curve is $-\frac{\alpha+u^*(1-\alpha)}{(1-u^*)(1-\alpha)}$. We further denote the “steady-state” share of poaching vacancies by $\phi^* = \frac{v_u^*}{v_u^*+v_\epsilon^*}$. To find the

³Note that based on our model approximation search effort of the employed can be expressed as a function of the number of unemployed $H_t = E_t - 0.78E_t^* = L_t - U_t - 0.78(L_t - U_t^*) = 0.22L_t + 0.78U_t^* - U_t \approx 0.27L_t - U_t$.

slope of the classical Beveridge curve, we need to understand the relationship between movements in y and z over the business cycle. In standard search models, movements in profitability of a match y reflect changes in productivity or demand driving the business cycle. It is natural to expect the profitability of poaching vacancies to be driven by similar factors. Therefore, we would expect y and z to have a common factor reflecting business-cycle fluctuations. We denote the elasticity of the co-movement between profitabilities by d_y , reflecting the ratio of their log standard deviations: $\ln\left(\frac{y}{y^*}\right) \propto d_y \ln\left(\frac{z}{z^*}\right)$. In fact, in our estimated model we estimated the factor x_t which is a common driver of both y_t and z_t and from the filtered estimates of the three shocks we can deduce a value for d_y of around 0.2. Then we can show that the slope of the classical Beveridge curve is:

$$-\phi^* \frac{\alpha + u^*(1 - \alpha)}{(1 - u^*)(1 - \alpha)} - (1 - \phi^*) \left(\frac{u^*}{0.27 - u^*} + \frac{1}{d_y \beta} \left(1 + \frac{\alpha + u^*(1 - \alpha)}{(1 - u^*)(1 - \alpha)} \right) \right).$$

The first term reflects movement in non-poaching vacancies in the adjusted Beveridge curve. The second term reflects the movements in search effort of the employed and the movements in the profitability of poaching vacancies over the business cycle.

To put some numbers to these slopes, we use the estimated parameters $\alpha = 0.16$, $\beta = 0.90$, the steady-state share of non-poaching vacancies $\phi^* = 0.45$,⁴ and the steady-state level of unemployment $u^* = 0.04$. For this calibration, the slope of the adjusted Beveridge curve is -0.33, consistent with the slope of the adjusted Beveridge curve shown in Figure 8. Assuming the estimated parameter $d_y = 0.15$, we also get the slope of the classical Beveridge curve right at -1, consistent with Figure 8 and the commonly accepted value of the slope in the literature. If the steady-state level of poaching vacancies were to increase to 0.85, as we have seen recently, then the Beveridge curve could have steepened to a slope of -1.4.

Figure 8 compares the joint behavior of unemployment and vacancies with the predictions of our calibrated theoretical model for the dual Beveridge curve. Instead of parameter values for B_u , B_e , s , z , and y , we input their estimated linear trend values for 2007 and 2019, two pre-recession peaks commonly used as reference points, and 2023, which is close to the end of observations at hand. The adjusted Beveridge curve in the right panel shifted down only mildly due to the reduced labor market dynamism, as captured by the decline in the trend separation rate. The classical Beveridge curve in the left panel both shifted outward and steepened its slope, due to the increase in steady-state profit-cost ratio z and the consequent expansion in the steady-state level of poaching vacancies. It expanded and steepened further for the estimated trend values of 2023, but we think it premature to project an indefinitely growing trend, and thus the estimate for 2019 represents a conservative estimate.

⁴To take a conservative approach, we use the estimated vacancy split that we observe prior to 2010.

7 Broader Implications and Future Directions

Our results are important for policy considerations, in particular, for monetary policy’s effect on unemployment. As argued by Figura and Waller (2022), a steeper Beveridge curve could imply that tighter monetary policy would result in a larger decline in vacancies corresponding to only a mild increase in the unemployment rate.

In this paper, we attribute the Beveridge curve puzzle to the disproportional expansion of poaching vacancies. Our estimates combined with a theoretical model indicate that the slope of the Beveridge curve has indeed steepened from -1 to at least -1.25 and possibly -1.4. This coefficient implies that a decline in the vacancy rate from 7% to 5% should correspond to an increase in the unemployment rate from 3.5 to at most 4.6 percent, and possibly 4.4 percent, as opposed to 4.9 percent previously. Another consequence of the expansion of poaching vacancies is the outward movement of the Beveridge curve, which suggests that a coexistence of a 6% vacancy rate (rather than 4% vacancy rate) with a 4% unemployment rate may be the new normal. Consequently, a monetary tightening in the 2020s is likely to lead to a larger decline in job openings corresponding to a milder increase in the unemployment rate, consistent with a notion of a “soft landing.”

The future is uncertain, however. The interpretation of the most recent behavior of the Beveridge curve depends on the reason for the expansion in poaching vacancies and whether it is likely to continue. Among the possible explanations are both factors that reduced the costs associated with filling vacancies and factors that increased their benefits to firms. The first set of factors includes the effects of the expansion of online job search tools and increased use of AI (Acemoglu et al, 2022), the expansion of available temporary and remote work (Bloom et al, 2023), and the expansion of the online gig economy (Stanton and Thomas, 2021). The second set of factors could include rising market concentration and markups (Autor et al, 2020, De Loecker et al, 2020) and the associated expansion of monopsony power of firms (Azar et al, 2019, Berger et al, 2022). If some of these factors are at play, the expansion of poaching vacancies could continue for as long as these trends continue. Therefore, more changes in monetary policy could be absorbed by poaching vacancies, with little impact on non-poaching vacancies and only a small increase in unemployment.

Alternatively, the expansion of poaching vacancies could be due to a reduction in mis-measurement: according to Davis et al. (2013), as of 2011, 42% of hires occurred at establishments that did not have any job openings. If those firms have gradually improved their reporting of vacancies that had not been reported previously, then the aggregate Beveridge curve has shifted outward, but there are limits to such an expansion. In this case, the Beveridge curve will stabilize at a new level and slope.

The main lesson from our exercise, however, is that instead of looking at the classical Beveridge curve and interpreting its increasingly chaotic movements, we should shift our attention to the adjusted Beveridge curve, which is unlikely to change much, and will therefore remain a good indicator of the state of the labor market going forward.

In addition to clarifying how to interpret the Beveridge curve, our model also offers a practical tool for

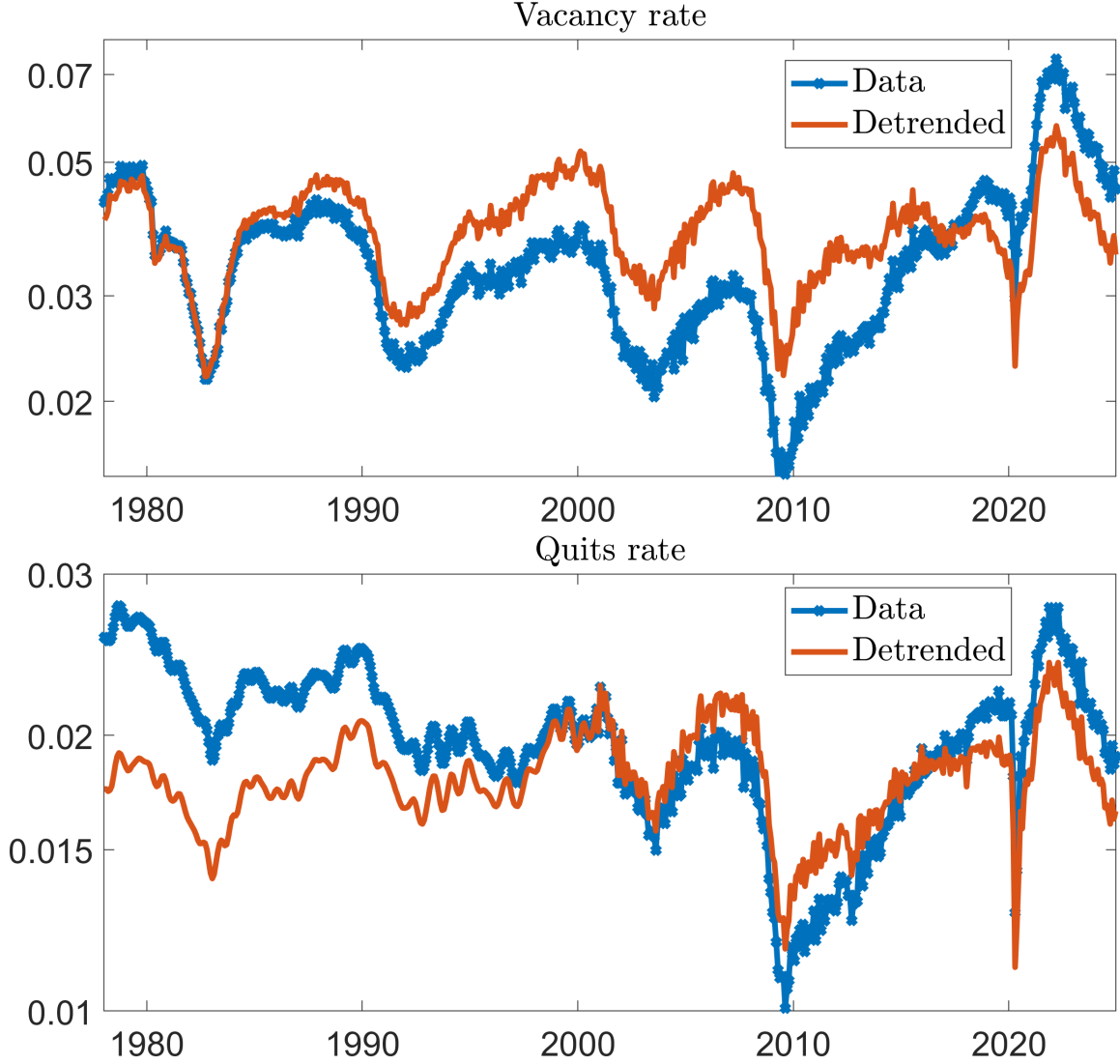


Figure 9: Detrended vacancies and quits.

disentangling structural and cyclical components in key labor market indicators. Because the estimated trends in poaching and non-poaching profitability reflect slow-moving changes in firm hiring strategies, we can use them to construct detrended versions of observed series such as vacancies and quits. Figure 9 shows the raw and adjusted vacancy and quits series after removing the structural trend components implied by our estimated model. This adjustment reveals that much of the increase in aggregate vacancies in recent years reflects long-term shifts in vacancy composition, rather than heightened cyclical labor demand. These adjusted series may serve as more reliable indicators for short-run policy analysis going forward.⁵

Another important takeaway point is that economists and statistical agencies need to put resources into

⁵While our adjusted vacancy and quit series are not intended as real-time policy tools, they provide a proof of concept for improving cyclical indicators by accounting for the composition of labor demand. Future work could explore operationalizing this adjustment using higher-frequency job posting data.

more and better measurement of the vacancy split, between vacancies targeting unemployed workers and vacancies designed for hiring workers that already have a job. Surveys of firms conducted by statistical agencies could ask the firms a question that would shed light on this issue and enable direct measurement of the vacancy split. Such measurement would both enable the development of better theoretical models and a better real-time assessment of the state of the labor market.

8 References

1. Acemoglu, Daron, Autor, David, Hazell, Jonathon, and Pascual Restrepo (2022) “Artificial Intelligence and Jobs: Evidence from Online Vacancies,” *Journal of Labor Economics*, 40 (S1), pp. S293–S340. DOI: <https://doi.org/10.1086/718327>
2. Afrouzi, Hassan, Blanco, Andrés, Drenik, Andrés, and Erik Hurst (2024) “A Theory of How Workers Keep Up With Inflation,” NBER Working Paper 33233.
3. Ahn, Hie Joo and Leland D. Crane (2020) “Dynamic Beveridge Curve Accounting,” BOG DP No. 2020-027, DOI: <https://doi.org/10.17016/FEDS.2020.027>
4. Ahn, Hie Joo, Hobijn, Bart and Ayşegül Şahin (2022) “The Dual U.S. Labor Market Uncovered,” mimeo, DOI: <https://doi.org/10.20955/wp.2022.021>
5. An, Sunbae and Frank Schorfheide (2007) “Bayesian analysis of DSGE models,” *Econometric Reviews*, 26 (2-4), 113-172. DOI: <https://doi.org/10.1080/07474930701220071>
6. Autor, David, Dorn, David, Katz, Lawrence F., Patterson, Christina, and John Van Reenen (2020) “The Fall of the Labor Share and the Rise of Superstar Firms.” *The Quarterly Journal of Economics*, 135 (2), pp. 645–709. DOI: <https://doi.org/10.1093/qje/qjaa004>
7. Azar, José, Marinescu, Ioana, and Marshall Steinbaum (2019) “Measuring Labor Market Power Two Ways” *AEA Papers and Proceedings*, 109, pp. 317–321. DOI: <https://doi.org/10.1257/pandp.20191068>
8. Barnichon, Régis (2010) “Building a composite Help-Wanted Index” *Economics Letters*, 109(3), pp. 175-178. DOI: <https://doi.org/10.1016/j.econlet.2010.08.029>
9. Berger, David W., Herkenhoff, Kyle F. and Simon Mongey (2022) “Labor Market Power” *American Economic Review*, 112(4), pp. 1147–1193. DOI: <https://doi.org/10.1257/aer.20191521>
10. Beveridge, William H. (1944) *Full Employment in a Free Society*. New York: W. W. Norton & Company, DOI: <https://doi.org/10.4324/9781315737348>
11. Birinci, Serdar, See, Kurt and Shu Lin Wee (2024) “Job Applications and Labour Market Flows” *Review of Economic Studies*, forthcoming. DOI: <https://doi.org/10.1093/restud/rdae064>

12. Blanchard, Olivier, Domash, Alex and Lawrence H. Summers (2022) “The Fed is wrong: Lower inflation is unlikely without raising unemployment,” *PIIE Realtime Economic Issues Watch*, August 2022, DOI: <http://dx.doi.org/10.2139/ssrn.4174601>
13. Bloom, Nicholas, Davis, Steven J., Hansen, Stephen, Lambert, Peter John, Sadun, Raffaella, and Bledi Taska (2023) “Remote Work across Jobs, Companies, and Space” *NBER Working Paper No. 31007*. DOI: <http://doi.org/10.3386/w31007>
14. Bonthuis, Boele, Jarvis, Valerie and Juuso Vanhala (2016) “Shifts in Euro Area Beveridge Curves and Their Determinants,” *IZA Journal of Labor Policy*, 5 (20), 1-17, DOI: <https://doi.org/10.1186/s40173-016-0076-7>
15. Broersma, Lourens, and Jan C. Van Ours (1999) “Job searchers, job matches and the elasticity of matching” *Labour Economics*, 6(1), pp. 77-93. DOI: [https://doi.org/10.1016/S0927-5371\(98\)00017-7](https://doi.org/10.1016/S0927-5371(98)00017-7)
16. Cheremukhin, A., Restrepo-Echavarria P. and A. Tutino (2020) “Targeted Search in Matching Markets.” *Journal of Economic Theory*, vol 185, pp. 1-43. DOI: <https://doi.org/10.1016/j.jet.2019.104956>
17. Cheremukhin, A. and Restrepo-Echavarria P.(2025) “An Information-based Theory of Monopsony Power.” *Dallas Fed Working Paper No. 2518*. DOI: <https://doi.org/10.24149/wp2518>
18. Crump, Richard K., Stefano Eusepi, Marc Giannoni, and Aysegül Şahin (2019): “A Unified Approach to Measuring u^* ,” *Brookings Papers on Economic Activity*. DOI: <https://doi.org/10.3386/w25930>
19. Davis, Steven J., Faberman, R. Jason and John C. Haltiwanger (2013) “The Establishment-Level Behavior of Vacancies and Hiring,” *The Quarterly Journal of Economics*, 128(2), 581-622, DOI: <https://doi.org/10.1093/qje/qjt002>
20. De Loecker, Jan, Eeckhout, Jan, and Gabriel Unger (2020) “The Rise of Market Power and the Macroeconomic Implications.” *The Quarterly Journal of Economics*, 135 (2), pp. 561–644. DOI: <https://doi.org/10.1093/qje/qjz041>
21. Diamond, Peter A. and Aysegül Şahin (2014) “Shifts in the Beveridge curve,” *Staff Reports 687*, FRB NY, DOI: <http://dx.doi.org/10.2139/ssrn.2488141>
22. Dow, J.C.R. and L.A. Dicks-Mireaux (1958) “The Excess Demand for Labour. A Study of Conditions in Great Britain, 1946-56.” *Oxford Economic Papers*, 10 (1), 1-33, DOI: <https://doi.org/10.1093/oxfordjournals.oep.a040791>
23. Ellieroth, Kathrin and Amanda M. Michaud (2024) “Quits, Layoffs, and Labor Supply.” *OIGI Working Papers 094*, Federal Reserve Bank of Minneapolis.
24. Elsby, Michael W. L., Gottfries, Axel, Michaels, Ryan and David Ratner (2025) “Vacancy Chains,” *Journal of Political Economy*, forthcoming. DOI: <https://doi.org/10.7910/DVN/HMRU7M>

25. Elsbey, Michael W. L., Michaels, Ryan and David Ratner (2015) “The Beveridge Curve: A Survey,” *Journal of Economic Literature*, 53(3), 571-630, DOI: <https://doi.org/10.1257/jel.53.3.571>
26. Faberman, R. Jason, Mueller, Andreas I., Şahin, Ayşegül and Giorgio Topa (2022) “Job Search Behavior Among the Employed and Non-Employed,” *Econometrica*, 90: 1743-1779, DOI: <https://doi.org/10.3982/ECTA18582>
27. Figura, Andrew, and Chris Waller (2022) “What does the Beveridge curve tell us about the likelihood of a soft landing?” BOG Fed Notes, July 2022, DOI: <https://doi.org/10.17016/2380-7172.3190>
28. Fujita, Shigeru and Makoto Nakajima (2016) “Worker flows and job flows: A quantitative investigation,” *Review of Economic Dynamics*, vol. 22, pp. 1-20, DOI: <https://doi.org/10.1016/j.red.2016.06.001>
29. Fujita, Shigeru and Moscarini, Giuseppe and Fabien Postel-Vinay (2024) “Measuring Employer-to-Employer Reallocation,” *American Economic Journal: Macroeconomics*, 16(3), pp. 1-51, DOI: <https://doi.org/10.1257/mac.20210076>
30. Geweke, J. (1999). “Using simulation methods for bayesian econometric models: inference, development and communication,” *Econometric Reviews*, 18 (1), 1–126. DOI: <https://doi.org/10.1080/07474939908800428>
31. Gottfries, Nils and Karolina Stadin (2024). “The Beveridge Curve, Matching, and Labour Market Flows: A Reinterpretation,” CESifo Working Paper Series 7689, CESifo.
32. Hall, Robert E. and Marianna Kudlyak (2020) “Job-Finding and Job-Losing: A Comprehensive Model of Heterogeneous Individual Labor-Market Dynamics,” FRB SF WP No. 2019-05, DOI: <https://doi.org/10.24148/wp2019-05>
33. Hobijn, Bart and Ayşegül Şahin (2012) “Beveridge Curve Shifts across Countries since the Great Recession,” FRB SF WP No. 2012-24, DOI: <https://doi.org/10.24148/wp2012-24>
34. Lubik, Thomas A. (2021) “Revisiting the Beveridge Curve: Why has it shifted so Dramatically,” FRB Richmond, Economic Brief No. 21-36, October.
35. Menzio, Guido and Shouyong Shi (2011) “Efficient Search on the Job and the Business Cycle,” *Journal of Political Economy*, 119 (3), pp. 468-510. DOI: <https://doi.org/10.1086/660864>
36. Mercan, Yusuf and Benjamin Schoefer (2020) “Jobs and Matches: Quits, Replacement Hiring, and Vacancy Chains,” *American Economic Review: Insights*, 2 (1), pp. 104-124. DOI: <https://doi.org/10.1257/aeri.20190023>
37. Molloy, Raven, Christopher L. Smith, Riccardo Trezzi, and Aabigail Wozniak (2016): “Understanding Declining Fluidity in the U.S. Labor Market,” *Brookings Papers on Economic Activity*. DOI: <https://doi.org/10.1353/eca.2016.0015>

38. Mongey, Simon and Jeff Horwich (2024): “Fewer openings, harder to get hired: U.S. labor market likely softer than it appears” Federal Reserve Bank of Minneapolis article, September 5, 2024.
39. Mortensen, Dale T. and Christopher A. Pissarides (1994) “Job Creation and Job Destruction in the Theory of Unemployment,” *Review of Economic Studies*, 61(3), 397-415, DOI: <https://doi.org/10.2307/2297896>
40. Pissarides, Christopher A. and Barbara Petrongolo (2001) “Looking into the Black Box: A Survey of the Matching Function,” *Journal of Economic Literature*, 39(2), 390-431, DOI: <https://doi.org/10.1257/jel.39.2.390>
41. Pissarides, Christopher A. (1985). “Short-Run Equilibrium Dynamics of Unemployment, Vacancies, and Real Wages.” *American Economic Review*, 75(4), pp. 676-690. DOI: <https://www.jstor.org/stable/1821347>
42. Pissarides, Christopher A. (2000). *Equilibrium Unemployment Theory*. 2nd ed., Cambridge, MA, MIT Press.
43. Qiu, Xincheng (2022) “Vacant Jobs” University of Pennsylvania, unpublished manuscript.
44. Rodgers, William M. and Alice L. Kassens (2022) “What Does the Beveridge Curve Tell Us about the Labor Market Recovery?” FRB SL, On The Economy Blog, July 2022.
45. Şahin, Aysegül, Song, Joseph, Topa, Giorgio and Giovanni L. Violante (2014) “Mismatch Unemployment” *American Economic Review*, 104(11), pp. 3529-3564. DOI: <https://doi.org/10.1257/aer.104.11.3529>
46. Stanton, Christopher T. and Catherine Thomas (2021) “Who Benefits from Online Gig Economy Platforms?” NBER Working paper 29477. DOI: <https://doi.org/10.3386/w29477>

Appendix A: Full Model

Main equations for endogenous variables:

- (1) $m_t^u = B_t^{u,tr} u_t^\alpha v_{u,t}^{1-\alpha} \left(1 + A_u \left(\frac{v_{\varepsilon,t}}{v_{u,t}}\right)^\gamma\right) + B_L n_t^\psi v_t^{1-\psi}$ matching of unemployed
- (2) $m_t^\varepsilon = B_t^{\varepsilon,tr} h_t^\beta v_{\varepsilon,t}^{1-\beta} \left(1 + A_\varepsilon \left(\frac{v_{u,t}}{v_{\varepsilon,t}}\right)^\gamma\right)$ matching of employed
- (3) $v_{u,t} + v_{\varepsilon,t} = v_t$ vacancy split
- (4) $h_t = e_t - \xi_t e_t^*$ search effort of employed
- (5) $e_t + u_t = 1$ labor force identity
- (6) $e_{t+1} \delta_{l,t} = e_t (1 - s_t) + m_t^u$ evolution of employment
- (7) $v_{u,t} = m_t^u y_t$ free entry of non-poaching vacancies
- (8) $v_{\varepsilon,t} = m_t^\varepsilon z_t$ free entry of poaching vacancies

Exogenous variables of the model:

- (9) $s_t = s_t^{tr} \exp \varphi_{1t}$ separation shock
- (10) $y_t = y_t^{tr} \exp(d_y x_t) \exp \varphi_{2t}$ low skill productivity shock
- (11) $z_t = z_t^{tr} \exp x_t \exp \varphi_{3t}$ high skill productivity shock
- (12) $\xi_t = \xi_0 \exp \varphi_{4t}$ share of ss employed that do not search
- (13) $\delta_{l,t} = \delta_{l0} \exp \varphi_{5t}$ growth rate of labor force
- (14) $n_t = n_0 \exp \varphi_{6t}$ evolution of not in the labor force
- (15) $e_t^* = e_0^* \exp \varphi_{7t}$ evolution of hp-filtered employment

Log-linearized version of the model (relative to trend, to be described below):

- (1) $\hat{m}_t^u = \alpha \hat{u}_t + (1 - \alpha) \hat{v}_{u,t} + c_u \gamma (\hat{v}_{\varepsilon,t} - \hat{v}_{u,t}) + b_L (\psi \hat{n}_t + (1 - \psi) \hat{v}_t)$
- (2) $\hat{m}_t^\varepsilon = \beta \hat{h}_t + (1 - \beta) \hat{v}_{\varepsilon,t} + c_\varepsilon \gamma (\hat{v}_{u,t} - \hat{v}_{\varepsilon,t})$
- (3) $\phi \hat{v}_{u,t} + (1 - \phi) \hat{v}_{\varepsilon,t} = \hat{v}_t$ vacancy split $\phi = \frac{v_u}{v}$ steady state
- (4) $\hat{h}_t = \frac{1}{1-\xi_0} \hat{e}_t - \frac{\xi_0}{1-\xi_0} (\hat{\xi}_t + \hat{e}_t^*)$ search effort of employed
- (5) $(1 - u_0) \hat{e}_t + u_0 \hat{u}_t = 0$ labor force identity
- (6) $\hat{e}_{t+1} + \hat{\delta}_{l,t} = (1 - s_0) \hat{e}_t - s_0 \hat{s}_t + s_0 \hat{m}_t^u$ evolution of employment
- (7) $\hat{v}_{u,t} = \hat{m}_t^u + \hat{y}_t$ free entry of non-poaching vacancies
- (8) $\hat{v}_{\varepsilon,t} = \hat{m}_t^\varepsilon + \hat{z}_t$ free entry of poaching vacancies
- (9) $\hat{s}_t = \varphi_{1t}$ separation shock
- (10) $\hat{y}_t = d_y x_t + \varphi_{2t}$ low skill productivity shock
- (11) $\hat{z}_t = x_t + \varphi_{3t}$ high skill productivity shock

$$(12) \quad \widehat{\xi}_t = \varphi_{4t} \quad \text{share of ss employed that do not search}$$

$$(13) \quad \widehat{\delta}_{l,t} = \varphi_{5t} \quad \text{growth rate of labor force}$$

$$(14) \quad \widehat{n}_t = \varphi_{6t} \quad \text{evolution of not in the labor force}$$

$$(15) \quad \widehat{e}_t^* = \varphi_{7t} \quad \text{evolution of hp-filtered employment}$$

Evolution of shocks:

$$x_t = \rho_1^x x_{t-1} + \rho_2^x x_{t-2} + \sigma^x \varepsilon_t^x \quad \text{common component of productivity in both sectors}$$

$$\varphi_{it} = \rho_i^\varphi \varphi_{it-1} + \sigma_i^\varphi \varepsilon_{it}^\varphi \quad \text{unknown shocks} \quad i = [1, 7]$$

Measurement equations:

$$(M1) \quad \widetilde{u}_t = \widehat{u}_t + \omega_{1t} \quad \text{unemployment rate}$$

$$(M2) \quad \widetilde{v}_t = \widehat{v}_t + \omega_{2t} \quad \text{vacancy rate}$$

$$(M3) \quad \widetilde{m}_t^u = \widehat{m}_t^u + \omega_{3t} \quad \text{hires-quits/LF, UE flow/LF}$$

$$(M4) \quad \widetilde{m}_t^\varepsilon = \widehat{m}_t^\varepsilon + \omega_{4t} \quad \text{quits/LF, EE flow/LF}$$

$$(M5) \quad \widetilde{s}_t = \widehat{s}_t + \omega_{5t} \quad \text{Layoffs/Employment, EU flow/Employment}$$

$$(M6) \quad \widetilde{e}_t = \widehat{m}_t^\varepsilon - \widehat{e}_t + \omega_{6t} \quad \text{E-E rate, version 0}$$

$$(M6') \quad \widetilde{e}_t = \widehat{m}_t^\varepsilon - \widehat{h}_t + \omega_{6t} \quad \text{E-E rate, version 1}$$

$$(M7) \quad \widetilde{\delta}_{l,t} = \widehat{\delta}_{l,t} + \omega_{7t} \quad \frac{LF_t}{LF_{t+1}} \quad \text{growth rate of labor force}$$

$$(M8) \quad \widetilde{n}_t = \widehat{n}_t + \omega_{8t} \quad \frac{N_t}{LF_t} \quad \text{out of the labor force rate}$$

$$(M9) \quad \widetilde{e}_t^* = \widehat{e}_t^* + \omega_{9t} \quad \text{hp-filtered (1000000) employment rate}$$

Measurement errors:

$$\omega_{jt} = \sigma_j^\omega \varepsilon_{jt}^\omega \quad \text{white noise measurement errors} \quad j = [1, 9]$$

Endogenous variables:

$$\widehat{e}_t, \widehat{u}_t, \widehat{v}_{u,t}, \widehat{v}_{\varepsilon,t}, \widehat{v}_t, \widehat{m}_t^u, \widehat{m}_t^\varepsilon, \widehat{h}_t, \widehat{s}_t, \widehat{y}_t, \widehat{z}_t, \widehat{\xi}_t, \widehat{\delta}_{l,t}, \widehat{n}_t, \widehat{e}_t^* \quad (15)$$

$$\widetilde{u}_t, \widetilde{v}_t, \widetilde{m}_t^u, \widetilde{m}_t^\varepsilon, \widetilde{s}_t, \widetilde{e}_t, \widetilde{\delta}_{l,t}, \widetilde{n}_t, \widetilde{e}_t^* \quad (9)$$

Exogenous variables: x_t, φ_{it}

41 equations, 41 variables, 17 shocks

Estimated parameters: $\alpha, \beta, \gamma, c_u, c_\varepsilon, \psi, b_L, \rho_1^x, \rho_2^x, \sigma^x, \rho_i^\varphi, \sigma_i^\varphi, \sigma_j^\omega$

Calibrated parameters: $\phi = 0.45, \xi_0 = 0.78, u_0 = 0.04, s_0 = 0.013, \sigma_i^\omega = 0.03$ for $i \in [1, 6]$,

$\sigma_i^\omega = 0.005$ for $i \in [7, 9]$

We allow for non-linear trends in the data series. More specifically, we assume that underlying shocks are the source of trends, and derive the correspondence to the trends in the data. We then estimate trends in the data from which we infer parameters of trends in the underlying shocks. We assume the following trends in shock variables:

$$\begin{aligned} B_t^{u,tr} &= B_0^u \exp(-a_u t) & B_t^{\varepsilon,tr} &= B_0^\varepsilon \exp(-a_\varepsilon t) \\ s_t^{tr} &= s_0 \exp(-a_s t) & y_t^{tr} &= y_0 \exp(a_y t) & z_t^{tr} &= z_0 \exp(a_z [t - \tau]_+) \end{aligned}$$

If we substitute these trends into equations (1 – 15), we can derive the following trend properties of observed variables:

$$\tilde{m}_{u,t}^{tr} = -a_s t \quad \tilde{s}_t^{tr} = -a_s t$$

Estimate $-a_s$ as average of the regression coefficients of $\ln m_{u,t}$ and $\ln s_t$ on a constant and time trend.

$$\tilde{u}_t^{tr} = (1 - u_0) \left(-a_s + \frac{a_u}{\alpha} + \frac{\alpha-1}{\alpha} a_y \right) t$$

Estimate $\left(-a_s + \frac{a_u}{\alpha} + \frac{\alpha-1}{\alpha} a_y \right)$ as $\frac{1}{(1-u_0)}$ of the regression coefficient $\ln u_t$ on a const and time trend.

$$\tilde{v}_t^{tr} = \phi(-a_s + a_y) t + (1 - \phi) \left(-\frac{1}{\beta} a_\varepsilon t + \frac{1}{\beta} a_z [t - \tau]_+ - u_0 \left(-a_s + \frac{a_u}{\alpha} + \frac{\alpha-1}{\alpha} a_y \right) t \right)$$

$$\tilde{m}_{\varepsilon,t}^{tr} = -\frac{1}{\beta} a_\varepsilon t + \frac{1-\beta}{\beta} a_z [t - \tau]_+ - u_0 \left(-a_s + \frac{a_u}{\alpha} + \frac{\alpha-1}{\alpha} a_y \right) t$$

We can use the parameters we already measured from other series to derive that

$$\frac{\tilde{v}_t^{tr} - \phi(-a_s + a_y)}{(1-\phi)} - \tilde{m}_{\varepsilon,t}^{tr} = a_z [t - \tau]_+$$

If we assume a value for a_y (we set it to 0), use the calibrated steady-state share of non-poaching vacancies ϕ , then we can directly measure the trend in $\ln z_t$ as the trend in the difference between the rescaled log vacancies and log EE matches. We estimate a break in this trend in τ = December 2010 and therefore obtain estimates of a_ε and a_z . Given all the trend parameters $a_s, a_u, a_y, a_\varepsilon, a_z, \tau$, we can subtract the trends from the measured series to obtain

$$\tilde{u}_t = \ln u_t - (1 - u_0) \left(-a_s + \frac{a_u}{\alpha} + \frac{\alpha-1}{\alpha} a_y \right) t$$

$$\tilde{v}_t = \ln v_t - \phi(-a_s + a_y) t - (1 - \phi) \left(-\frac{1}{\beta} a_\varepsilon t + \frac{1}{\beta} a_z [t - \tau]_+ - u_0 \left(-a_s + \frac{a_u}{\alpha} + \frac{\alpha-1}{\alpha} a_y \right) t \right)$$

$$\tilde{m}_t^u = \ln m_t^u - a_s t$$

$$\tilde{m}_t^\varepsilon = \ln m_t^\varepsilon + \frac{1}{\beta} a_\varepsilon t - \frac{1-\beta}{\beta} a_z [t - \tau]_+ + u_0 \left(-a_s + \frac{a_u}{\alpha} + \frac{\alpha-1}{\alpha} a_y \right) t$$

$$\tilde{s}_t = \ln s_t - a_s t$$

$$\tilde{e}e_t = \ln ee_t + \frac{1}{\beta} a_\varepsilon t - \frac{1-\beta}{\beta} a_z [t - \tau]_+ + u_0 \left(-a_s + \frac{a_u}{\alpha} + \frac{\alpha-1}{\alpha} a_y \right) t + \frac{u_0}{1-u_0} a_s t$$

$$\tilde{\delta}_{l,t} = \ln \delta_{l,t}$$

$$\tilde{n}_t = \ln n_t$$

$$\tilde{e}_t^* = \ln e_t^*$$

All of the series are then de-meanded to be consistent with a steady-state value of zero.

Appendix B: Identification

The log-linearized model (1 – 15) can be separated into the endogenous block, containing equations (1, 2, 3, 7, 8) and the exogenous block containing the rest of the equations. Because through equation (6) employment \hat{e}_t is the state variable of the model determined one period in advance, and through equation (5) the same is true for unemployment \hat{u}_t , and so the search effort \hat{h}_t is also exogenous through equation (4), they can be all substituted in to obtain the following system of equations.

$$\begin{aligned}
(1) \quad & (1 - \alpha - c_u \gamma) \hat{v}_{u,t} + c_u \gamma \hat{v}_{\varepsilon,t} = \hat{m}_{u,t} - \alpha \hat{u}_t - b_L \psi \hat{n}_t - b_L (1 - \psi) \hat{v}_t \\
(2) \quad & (1 - \beta - c_\varepsilon \gamma) \hat{v}_{\varepsilon,t} + c_\varepsilon \gamma \hat{v}_{u,t} = \hat{m}_{\varepsilon,t} + \beta \frac{u_0}{1-u_0} \frac{1}{1-\xi_0} \hat{u}_t + \beta \frac{\xi_0}{1-\xi_0} \hat{\xi}_t \\
(3) \quad & \phi \hat{v}_{u,t} + (1 - \phi) \hat{v}_{\varepsilon,t} = \hat{v}_t \\
(7) \quad & \hat{v}_{u,t} = \hat{m}_{u,t} + \hat{y}_t \\
(8) \quad & \hat{v}_{\varepsilon,t} = \hat{m}_{\varepsilon,t} + \hat{z}_t
\end{aligned}$$

This system can be written in matrix form as follows:

$$\begin{bmatrix} 1 - \alpha - \gamma c_u & \gamma c_u & 0 & 0 & 0 \\ \gamma c_\varepsilon & 1 - \beta - \gamma c_\varepsilon & 0 & 0 & -a_2 \\ \phi & 1 - \phi & 0 & 0 & 0 \\ 1 & 0 & -1 & 0 & 0 \\ 0 & 1 & 0 & -1 & 0 \end{bmatrix} \begin{bmatrix} v_u \\ v_\varepsilon \\ y \\ z \\ \xi \end{bmatrix} = \begin{bmatrix} -b_L \psi & -\alpha & -b_L(1 - \psi) & 1 & 0 \\ 0 & a_1 & 0 & 0 & 1 \\ 0 & 0 & 1 & 0 & 0 \\ 0 & 0 & 0 & 1 & 0 \\ 0 & 0 & 0 & 0 & 1 \end{bmatrix} \begin{bmatrix} n \\ u \\ v \\ m_u \\ m_\varepsilon \end{bmatrix}$$

where we denoted $a_1 = \beta \frac{u_0}{1-u_0} \frac{1}{1-\xi_0}$ $a_2 = \beta \frac{\xi_0}{1-\xi_0}$. This form can be used to understand the mapping from observables to unobservables. Inverting the system (and assuming $b_L = 0$, we obtain:

$$\begin{bmatrix} v_u \\ v_\varepsilon \\ y \\ z \\ \xi \end{bmatrix} = \begin{bmatrix} 0 & -\alpha(1 - \phi)D & -\gamma c_u D & D(1 - \phi) & 0 \\ 0 & \alpha \phi D & (1 - \alpha - \gamma c_u)D & -\phi D & 0 \\ 0 & -\alpha(1 - \phi)D & -\gamma c_u D & D(1 - \phi) - 1 & 0 \\ 0 & \alpha \phi D & (1 - \alpha - \gamma c_u)D & -\phi D & -1 \\ 0 & \frac{\alpha G - a_1}{a_2} D & \frac{F}{a_2} D & -\frac{G}{a_2} D & -\frac{1}{a_2} D \end{bmatrix} \begin{bmatrix} n \\ u \\ v \\ m_u \\ m_\varepsilon \end{bmatrix}$$

where $D = \frac{1}{(1-\phi)(1-\alpha)-\gamma c_u}$, $F = ((1-\beta)(1-\alpha) - \gamma c_u(1-\beta) - \gamma c_\varepsilon(1-\alpha))$, $G = ((1-\beta)\phi - \gamma c_\varepsilon)$

From this expression we can deduce how the vacancy split (on the left) and parameters are identified from properties of the data (on the right). The series for both types of vacancies, v_u and v_ε , and the shock y only depend on the number of matches made by unemployed, the number of unemployed and the total number of vacancies. Since vacancies and unemployment are quite volatile compared with the matching rate for the unemployed, the estimated model tends to give low estimates of parameters c_u and α . It is notable that none of the variables v_u, v_ε, y, z depend on the behavior of out of the labor force, or the parameters $\beta, c_\varepsilon, \psi, b_L$. The high estimate of β is likely determined by the fact that it only enters in the last line determining the search effort of the employed always in the form $1 - \beta$. Making β close to 1, and therefore this value close

to zero, minimizes the variance of the unobserved search effort.

The system of 5 equations can also be written to determine endogenous variables as a function of exogenous variables:

$$\begin{bmatrix} (1 - \alpha - c_u \gamma) & c_u \gamma & b_L (1 - \psi) & -1 & 0 \\ c_\varepsilon \gamma & (1 - \beta - c_\varepsilon \gamma) & 0 & 0 & -1 \\ \phi & 1 - \phi & -1 & 0 & 0 \\ 1 & 0 & 0 & -1 & 0 \\ 0 & 1 & 0 & 0 & -1 \end{bmatrix} \begin{bmatrix} v_u \\ v_\varepsilon \\ v \\ m_u \\ m_\varepsilon \end{bmatrix} = \begin{bmatrix} -\alpha & 0 & 0 & 0 & -b_L \psi \\ a_1 & 0 & 0 & a_2 & 0 \\ 0 & 0 & 0 & 0 & 0 \\ 0 & 1 & 0 & 0 & 0 \\ 0 & 0 & 1 & 0 & 0 \end{bmatrix} \begin{bmatrix} u \\ y \\ z \\ \xi \\ n \end{bmatrix}$$

This system can also be inverted in closed form (we again assume $b_L = 0$ for simplicity):

$$\begin{bmatrix} v_u \\ v_\varepsilon \\ v \\ m_u \\ m_\varepsilon \end{bmatrix} = E \cdot \begin{bmatrix} \alpha(\beta + \gamma c_\varepsilon) - a_1 \gamma c_u & \beta + \gamma c_\varepsilon & \gamma c_u & \gamma c_u & 0 \\ \alpha \gamma c_\varepsilon - a_1(\alpha + \gamma c_u) & \gamma c_\varepsilon & \alpha + \gamma c_u & \alpha + \gamma c_u & 0 \\ \alpha(\beta + \gamma c_\varepsilon) - a_1(\alpha(1 - \phi) + \gamma c_u) & \beta \phi + \gamma c_\varepsilon & \gamma c_u + \alpha(1 - \phi) & \gamma c_u + \alpha(1 - \phi) & 0 \\ \alpha \gamma c_\varepsilon - a_1 \gamma c_u & \beta(1 - \alpha - \gamma c_u) + \gamma c_\varepsilon(1 - \alpha) & \gamma c_u & \gamma c_u & 0 \\ \alpha \gamma c_\varepsilon - a_1(\alpha + \gamma c_u) & \gamma c_\varepsilon & \alpha(1 - \beta - \gamma c_\varepsilon) + \gamma c_u(1 - \beta) & \alpha + \gamma c_u & 0 \end{bmatrix} \begin{bmatrix} u \\ y \\ z \\ -a_2 \xi \\ n \end{bmatrix}$$

where we denoted $E = \frac{1}{\alpha\beta + \beta\gamma c_u + \alpha\gamma c_\varepsilon}$. When c_ε and c_u approach 0, this further simplifies to:

$$\begin{bmatrix} v_u \\ v_\varepsilon \\ v \\ m_u \\ m_\varepsilon \end{bmatrix} = \begin{bmatrix} 1 & \frac{1}{\alpha} & 0 & 0 & 0 \\ -\frac{a_1}{\beta} & 0 & \frac{1}{\beta} & \frac{1}{\beta} & 0 \\ 1 - \frac{a_1(1-\phi)}{\beta} & \frac{\phi}{\alpha} & \frac{1-\phi}{\beta} & \frac{1-\phi}{\beta} & 0 \\ 0 & \frac{1-\alpha}{\alpha} & 0 & 0 & 0 \\ -\frac{a_1}{\beta} & 0 & \frac{1-\beta}{\beta} & \frac{1}{\beta} & 0 \end{bmatrix} \begin{bmatrix} u \\ y \\ z \\ -a_2 \xi \\ n \end{bmatrix}$$

It is clear that v_u and m_u are driven only by u and y . The parameter c_u controls the spillovers from z . The remaining vacancies, as well as matches of the employed, are in addition affected by z and ξ , and the strength of these effects are controlled by parameters β and c_ε . Parameter ϕ enters to determine total vacancies as the sum of the two types.

Appendix C: Estimation Results

In Figure 10 and Tables 6 and 7 we report the estimates of parameters. We estimate α to be low (in the 0.1-0.2 range) and β to be high (in the 0.8-1 range). Figures 11-12 report the fit to the data and the estimated shocks for two most important specifications, when data are taken from the CPS or from JOLTS, and Figure 3 shows the estimates of the vacancy split and profit-cost ratios, with averages and confidence bounds over all six estimated specifications. All specifications find that the share of poaching vacancies increased after 2010 and that this was driven by an increase in the profit-cost ratio for poaching vacancies. Estimates of parameters with restrictions on the matching functions are presented in Tables 8 and 9.

We estimate the same specification of the model for 12 two-digit sectors of the economy using the JOLTS version of the data (as the only one available for the sectors). Estimates of parameters, reported in Figure 13, show that estimates for the sectors are largely consistent with the aggregate estimates. The behavior of the underlying shocks, illustrated for the manufacturing, business services, trade, transportation and utilities, and health and education services in Figures 14-17 show the same general pattern for the shocks as for the overall economy.

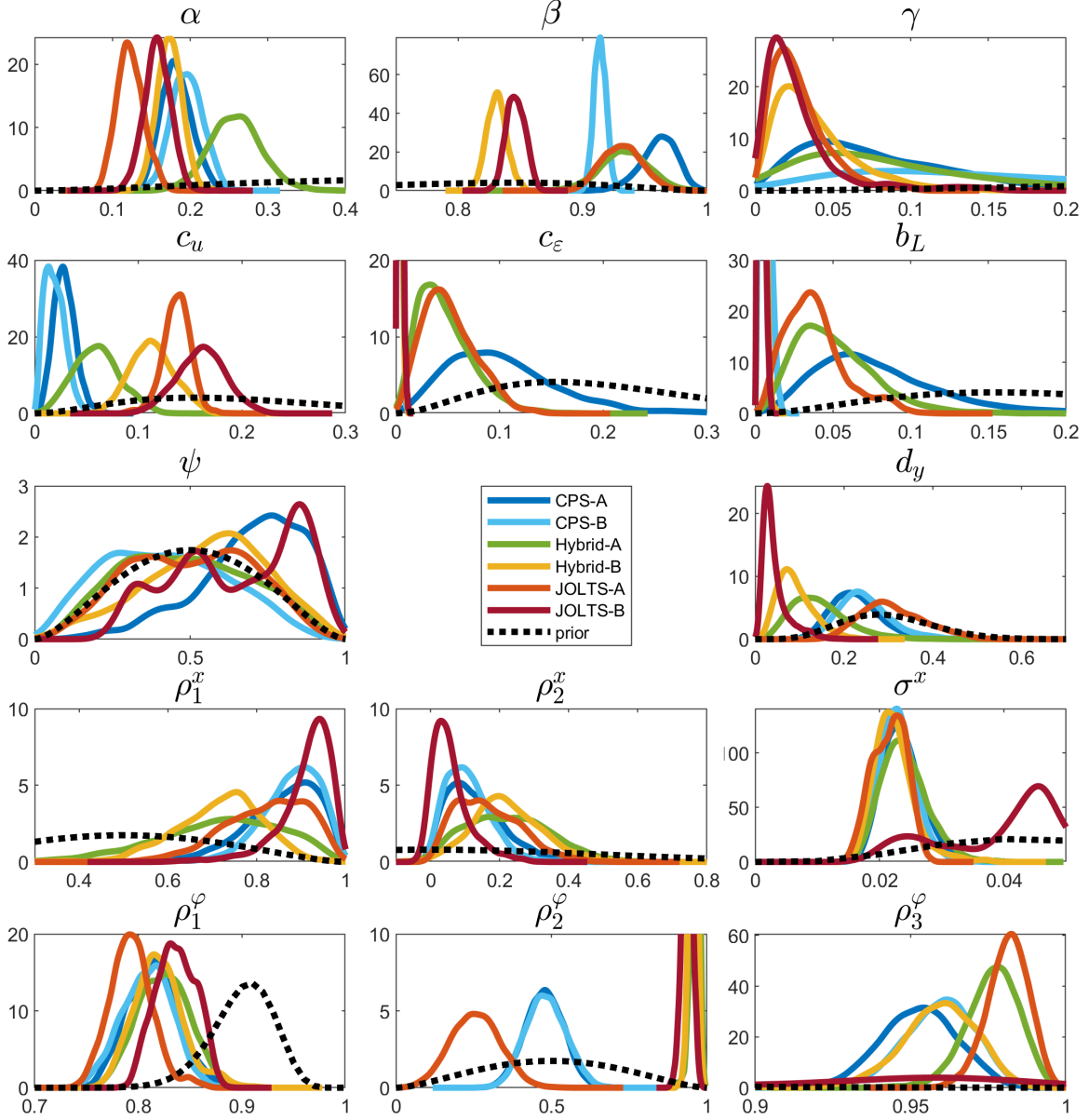


Figure 10: Prior and Posterior Estimates of Parameters for 6 estimation setups.

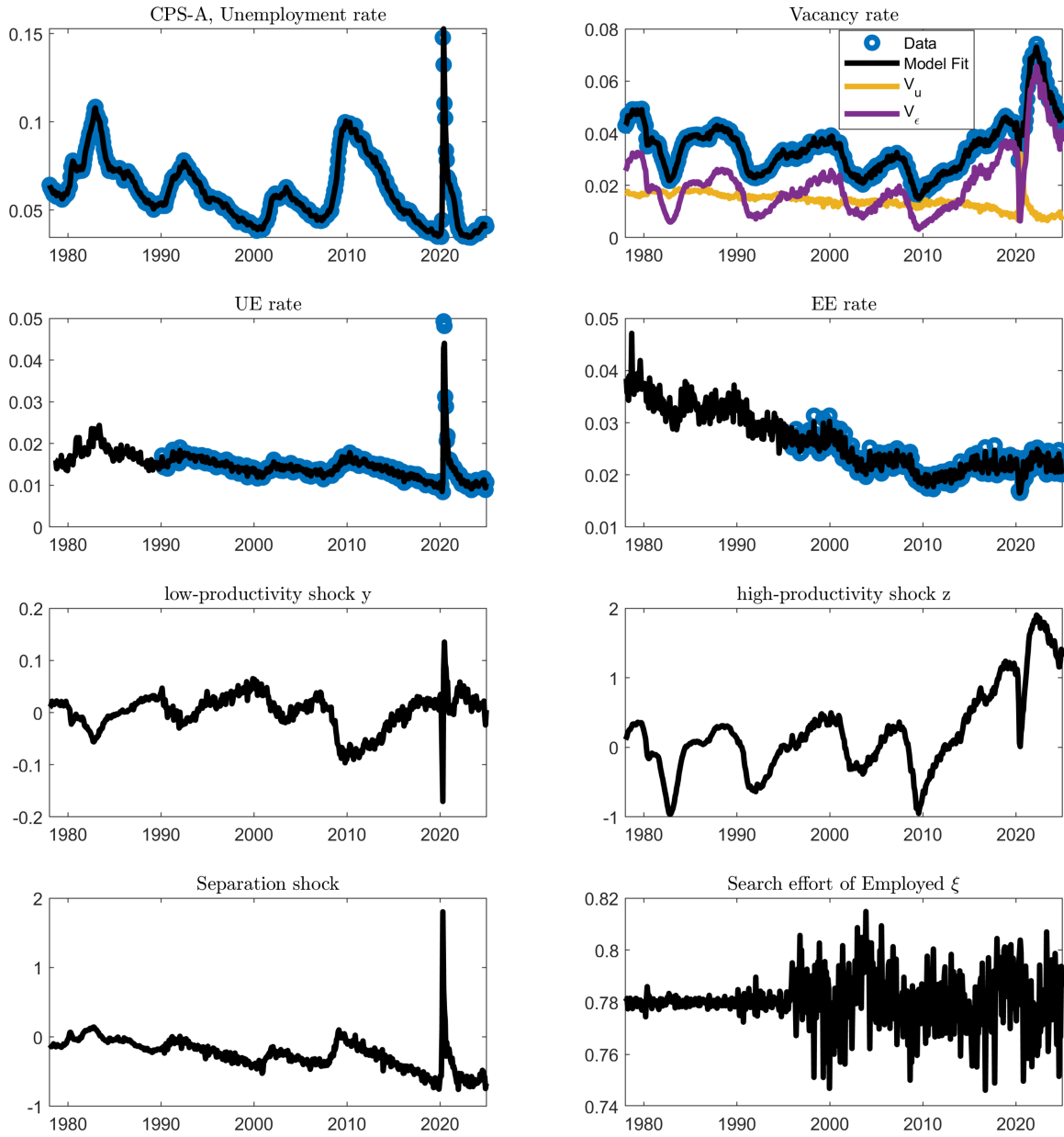


Figure 11: Model Fit and Shocks for CPS-A estimation.

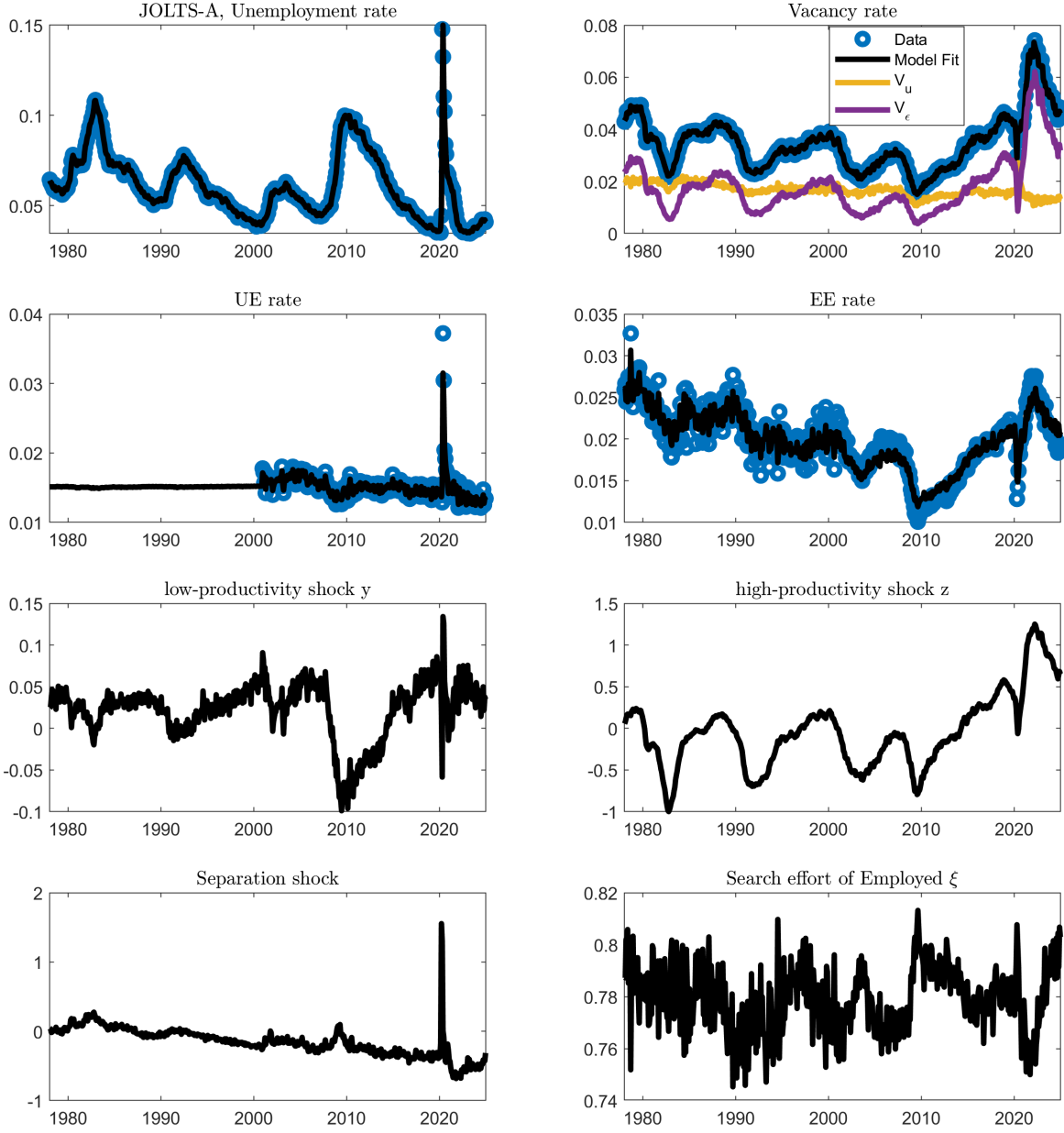


Figure 12: Model Fit and Shocks for JOLTS-A estimation.

Table 6: Parameter estimates of the DV model in the CPS-A specification

Parameter	Prior			Posterior		
	mean	st.dev.	mode	mean	st. dev.	conf. int. [5-95]
α	0.5	0.2	0.179	0.182	0.020	[0.150, 0.214]
β	0.8	0.1	0.967	0.961	0.012	[0.938, 0.984]
γ	0.5	0.2	0.106	0.079	0.036	[0.008, 0.148]
c_u	0.2	0.1	0.026	0.029	0.008	[0.011, 0.045]
c_ϵ	0.2	0.1	0.065	0.102	0.029	[0.018, 0.178]
ψ	0.5	0.2	0.74	0.70	0.09	[0.44, 0.97]
b_L	0.2	0.1	0.091	0.078	0.031	[0.016, 0.135]
d_y	0.5	0.2	0.20	0.23	0.06	[0.14, 0.32]
ρ^x	0.5	0.2	0.90	0.86	0.08	[0.74, 0.98]
ρ_2^x	0.0	0.5	0.08	0.13	0.08	[0.01, 0.25]
σ^x	0.05	0.02	0.024	0.024	0.004	[0.018, 0.029]
ρ_1^φ	0.9	0.03	0.81	0.81	0.012	[0.77, 0.85]
ρ_2^φ	0.5	0.2	0.47	0.48	0.05	[0.38, 0.58]
ρ_3^φ	0.5	0.2	0.955	0.953	0.015	[0.932, 0.973]
ρ_4^φ	0.5	0.2	0.15	0.13	0.05	[0.05, 0.21]
ρ_5^φ	0.1	0.03	0.08	0.08	0.02	[0.04, 0.12]
ρ_6^φ	0.9	0.03	0.950	0.948	0.010	[0.931, 0.965]
ρ_7^φ	0.9	0.03	0.928	0.936	0.011	[0.915, 0.960]
σ_1^φ	0.1	0.05	0.118	0.118	0.005	[0.111, 0.126]
σ_2^φ	0.05	0.02	0.016	0.017	0.002	[0.015, 0.020]
σ_3^φ	0.1	0.05	0.081	0.082	0.004	[0.075, 0.090]
σ_4^φ	0.01	0.005	0.016	0.017	0.001	[0.015, 0.019]
σ_6^φ	0.005	0.002	0.005	0.005	0.0002	[0.005, 0.006]

Notes: The priors for α , β , γ , c_u , c_ϵ , ψ , ρ^x , ρ_i^φ were drawn from a beta distribution with support on the interval $[0, 1]$, priors for b_L and d_y were drawn from a gamma distribution with positive support, priors for σ^x and σ_i^φ were drawn from an inverse gamma distribution with positive support, prior for ρ_2^x was drawn from a normal distribution.

Table 7: Parameter estimates of the DV model in the JOLTS-A specification

Parameter	Prior			Posterior		
	mean	st.dev.	mode	mean	st. dev.	conf. int. [5-95]
α	0.5	0.2	0.119	0.123	0.042	[0.094, 0.150]
β	0.8	0.1	0.935	0.932	0.017	[0.906, 0.959]
γ	0.5	0.2	0.021	0.028	0.020	[0.003, 0.053]
c_u	0.2	0.1	0.139	0.137	0.013	[0.115, 0.157]
c_ϵ	0.2	0.1	0.028	0.051	0.021	[0.011, 0.091]
ψ	0.5	0.2	0.421	0.501	0.098	[0.198, 0.820]
b_L	0.2	0.1	0.021	0.038	0.017	[0.008, 0.067]
d_y	0.5	0.2	0.249	0.309	0.067	[0.197, 0.426]
ρ^x	0.5	0.2	0.775	0.820	0.086	[0.683, 0.965]
ρ_2^x	0.0	0.5	0.215	0.166	0.085	[0.026, 0.307]
σ^x	0.05	0.02	0.024	0.022	0.003	[0.017, 0.026]
ρ_1^φ	0.9	0.03	0.782	0.793	0.022	[0.757, 0.823]
ρ_2^φ	0.5	0.2	0.235	0.255	0.319	[0.127, 0.383]
ρ_3^φ	0.5	0.2	0.983	0.981	0.029	[0.971, 0.992]
ρ_4^φ	0.5	0.2	0.540	0.552	0.060	[0.480, 0.628]
ρ_5^φ	0.1	0.03	0.273	0.283	0.010	[0.230, 0.328]
ρ_6^φ	0.9	0.03	0.940	0.943	0.008	[0.928, 0.959]
ρ_7^φ	0.9	0.03	0.937	0.936	0.017	[0.917, 0.956]
σ_1^φ	0.1	0.05	0.102	0.102	0.003	[0.097, 0.107]
σ_2^φ	0.05	0.02	0.017	0.017	0.003	[0.014, 0.019]
σ_3^φ	0.1	0.05	0.054	0.054	0.007	[0.048, 0.059]
σ_4^φ	0.01	0.005	0.014	0.014	0.001	[0.013, 0.016]
σ_6^φ	0.005	0.002	0.005	0.005	0.0002	[0.005, 0.006]

Notes: The priors for α , β , γ , c_u , c_ϵ , ψ , ρ^x , ρ_i^φ were drawn from a beta distribution with support on the interval $[0, 1]$, priors for b_L and d_y were drawn from a gamma distribution with positive support, priors for σ^x and σ_i^φ were drawn from an inverse gamma distribution with positive support, prior for ρ_2^x was drawn from a normal distribution.

Table 8: Parameter estimates of the SMF model in the CPS-A specification

Parameter	Prior			Posterior		
	mean	st.dev.	mode	mean	st. dev.	conf. int. [5-95]
α	0.5	0.2	0.332	0.338	0.012	[0.315, 0.360]
ψ	0.5	0.2	0.982	0.974	0.016	[0.952, 0.996]
b_L	0.2	0.1	0.575	0.572	0.020	[0.534, 0.612]
d_y	0.5	0.2	0.341	0.362	0.218	[0.127, 0.573]
ρ^x	0.5	0.2	0.917	0.849	0.109	[0.701, 0.990]
ρ_2^x	0.0	0.5	0.052	0.100	0.103	[-0.031, 0.248]
ρ_1^φ	0.9	0.03	0.815	0.808	0.026	[0.769, 0.849]
ρ_2^φ	0.5	0.2	0.960	0.804	0.039	[0.530, 0.989]
ρ_3^φ	0.5	0.2	0.970	0.971	0.013	[0.956, 0.987]
ρ_4^φ	0.5	0.2	0.824	0.817	0.030	[0.765, 0.868]
ρ_5^φ	0.1	0.03	0.084	0.083	0.017	[0.047, 0.119]
ρ_6^φ	0.9	0.03	0.949	0.948	0.009	[0.930, 0.965]
ρ_7^φ	0.9	0.03	0.942	0.937	0.015	[0.917, 0.958]
σ^x	0.05	0.02	0.029	0.028	0.003	[0.020, 0.036]
σ_1^φ	0.1	0.05	0.117	0.118	0.004	[0.111, 0.124]
σ_2^φ	0.05	0.02	0.031	0.031	0.005	[0.020, 0.041]
σ_3^φ	0.1	0.05	0.052	0.054	0.005	[0.045, 0.063]
σ_4^φ	0.01	0.005	0.029	0.030	0.002	[0.027, 0.033]
σ_6^φ	0.005	0.002	0.005	0.005	0.0003	[0.005, 0.006]

Notes: The priors for α , ψ , ρ^x , ρ_i^φ were drawn from a beta distribution with support on the interval $[0, 1]$, priors for b_L and d_y were drawn from a gamma distribution with positive support, priors for σ^x and σ_i^φ were drawn from an inverse gamma distribution with positive support, prior for ρ_2^x was drawn from a normal distribution.

Table 9: Parameter estimates of the SMF model in the JOLTS-A specification

Parameter	Prior			Posterior		
	mean	st.dev.	mode	mean	st. dev.	conf. int. [5-95]
α	0.5	0.2	0.137	0.142	0.010	[0.130, 0.153]
ψ	0.5	0.2	0.989	0.985	0.016	[0.971, 0.999]
b_L	0.2	0.1	0.473	0.465	0.012	[0.441, 0.488]
d_y	0.5	0.2	0.451	0.375	0.059	[0.152, 0.578]
ρ^x	0.5	0.2	0.945	0.923	0.039	[0.864, 0.987]
ρ_2^x	0.0	0.5	0.021	0.031	0.040	[-0.045, 0.104]
ρ_1^φ	0.9	0.03	0.798	0.800	0.007	[0.772, 0.827]
ρ_2^φ	0.5	0.2	0.909	0.882	0.026	[0.788, 0.976]
ρ_3^φ	0.5	0.2	0.969	0.964	0.025	[0.943, 0.985]
ρ_4^φ	0.5	0.2	0.973	0.973	0.011	[0.958, 0.987]
ρ_5^φ	0.1	0.03	0.379	0.377	0.005	[0.374, 0.379]
ρ_6^φ	0.9	0.03	0.941	0.947	0.004	[0.926, 0.969]
ρ_7^φ	0.9	0.03	0.937	0.932	0.008	[0.910, 0.953]
σ^x	0.05	0.02	0.023	0.024	0.003	[0.020, 0.029]
σ_1^φ	0.1	0.05	0.101	0.101	0.003	[0.096, 0.107]
σ_2^φ	0.05	0.02	0.026	0.027	0.002	[0.021, 0.033]
σ_3^φ	0.1	0.05	0.038	0.038	0.003	[0.033, 0.044]
σ_4^φ	0.01	0.005	0.017	0.018	0.001	[0.016, 0.020]
σ_6^φ	0.005	0.002	0.005	0.005	0.0001	[0.005, 0.006]

Notes: The priors for α , ψ , ρ^x , ρ_i^φ were drawn from a beta distribution with support on the interval $[0, 1]$, priors for b_L and d_y were drawn from a gamma distribution with positive support, priors for σ^x and σ_i^φ were drawn from an inverse gamma distribution with positive support, prior for ρ_2^x was drawn from a normal distribution.

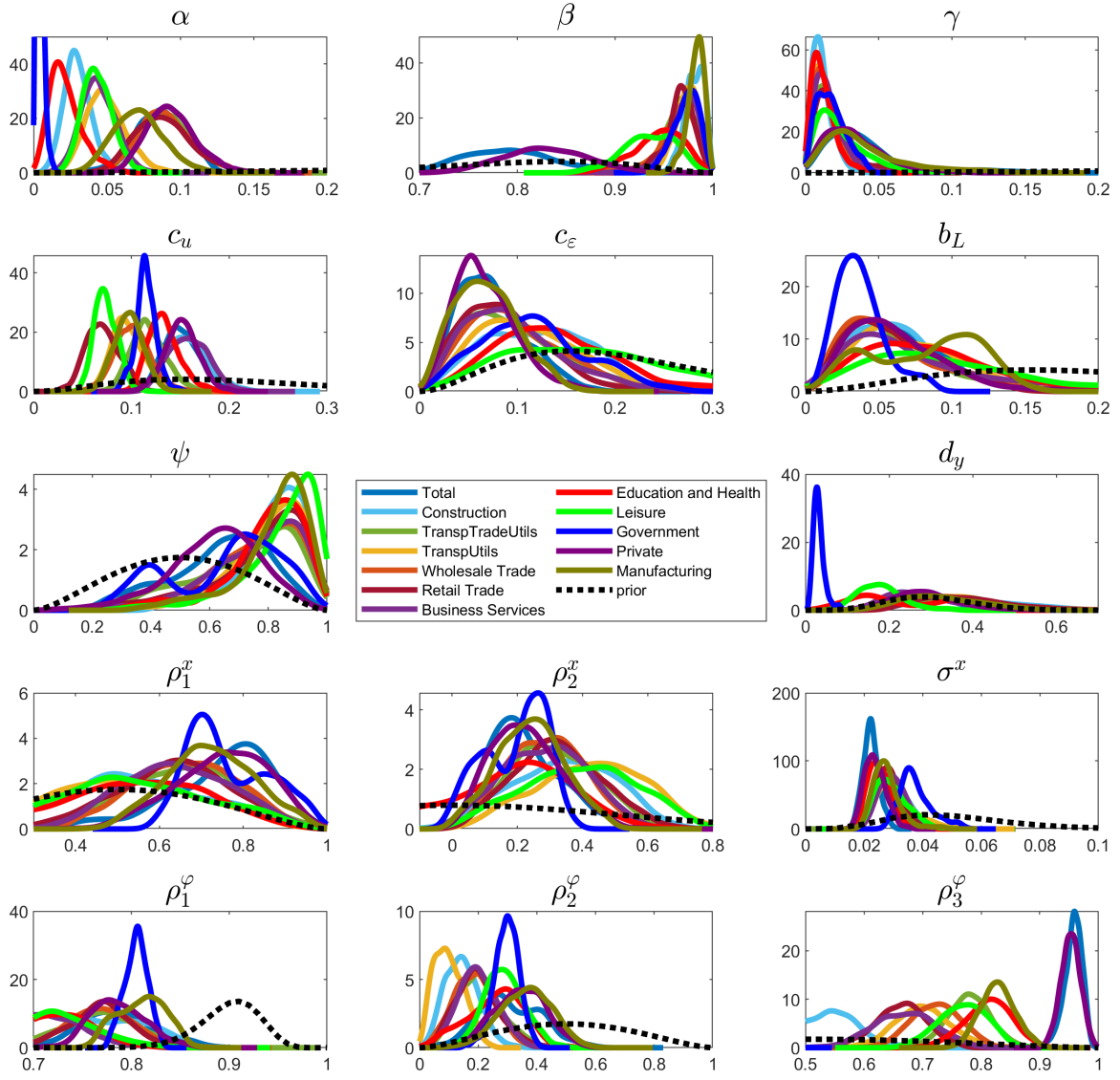


Figure 13: Prior and Posterior Estimates of Parameters for 12 sectors of the economy using JOLTS data.

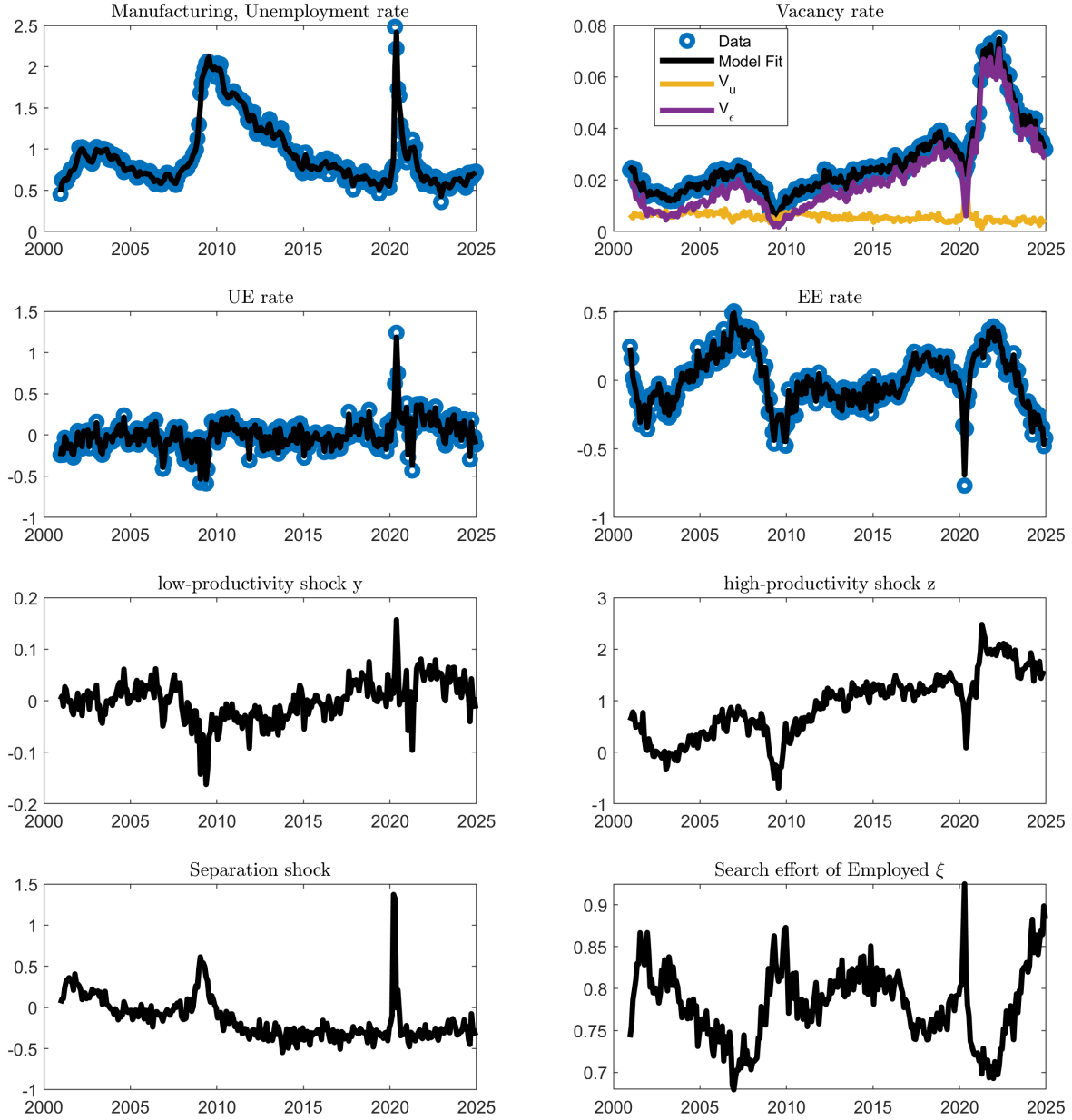


Figure 14: Model Fit and Shocks for Manufacturing Sector estimation.

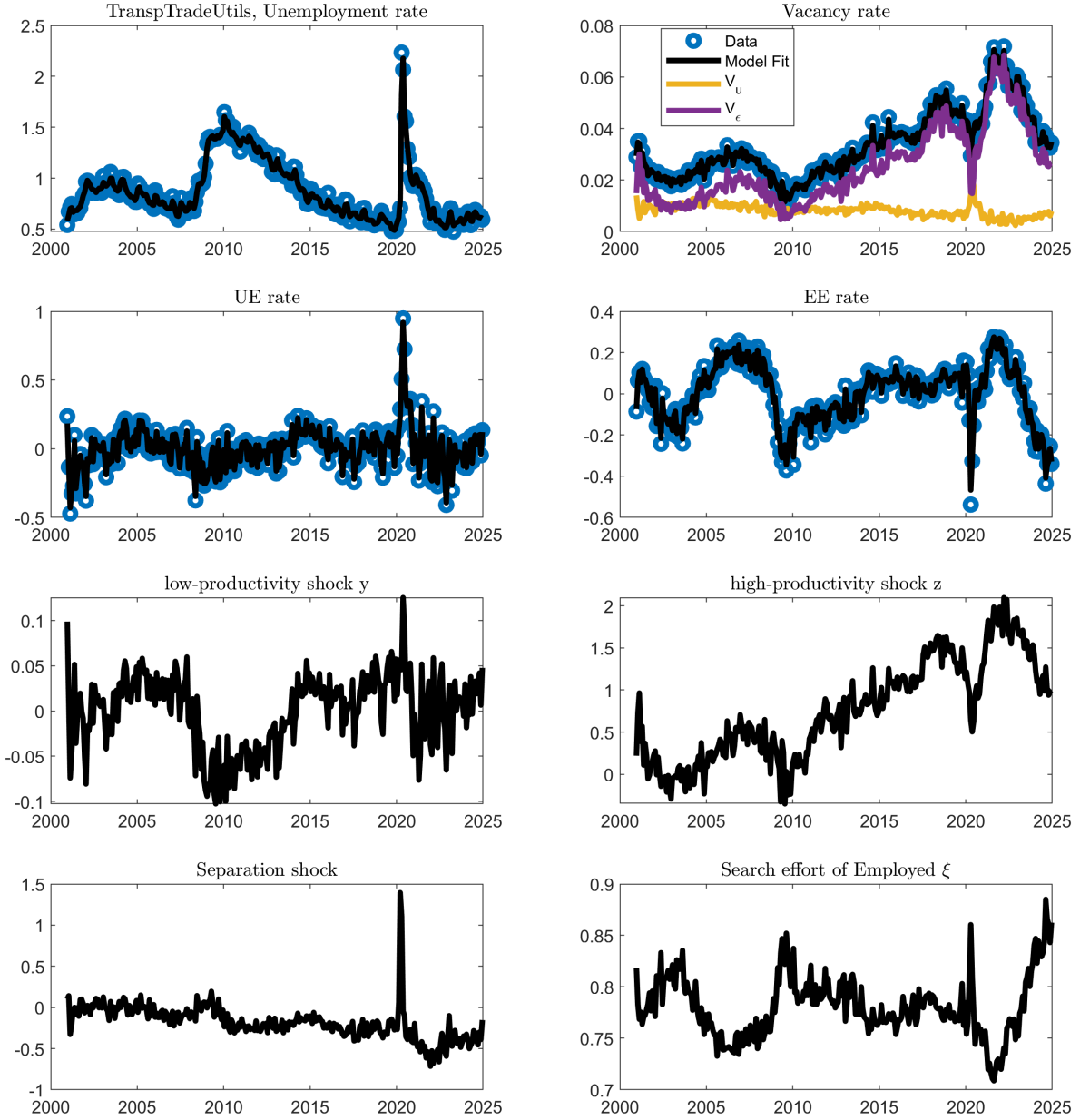


Figure 15: Model Fit and Shocks for Trade, Transportation and Utilities estimation.

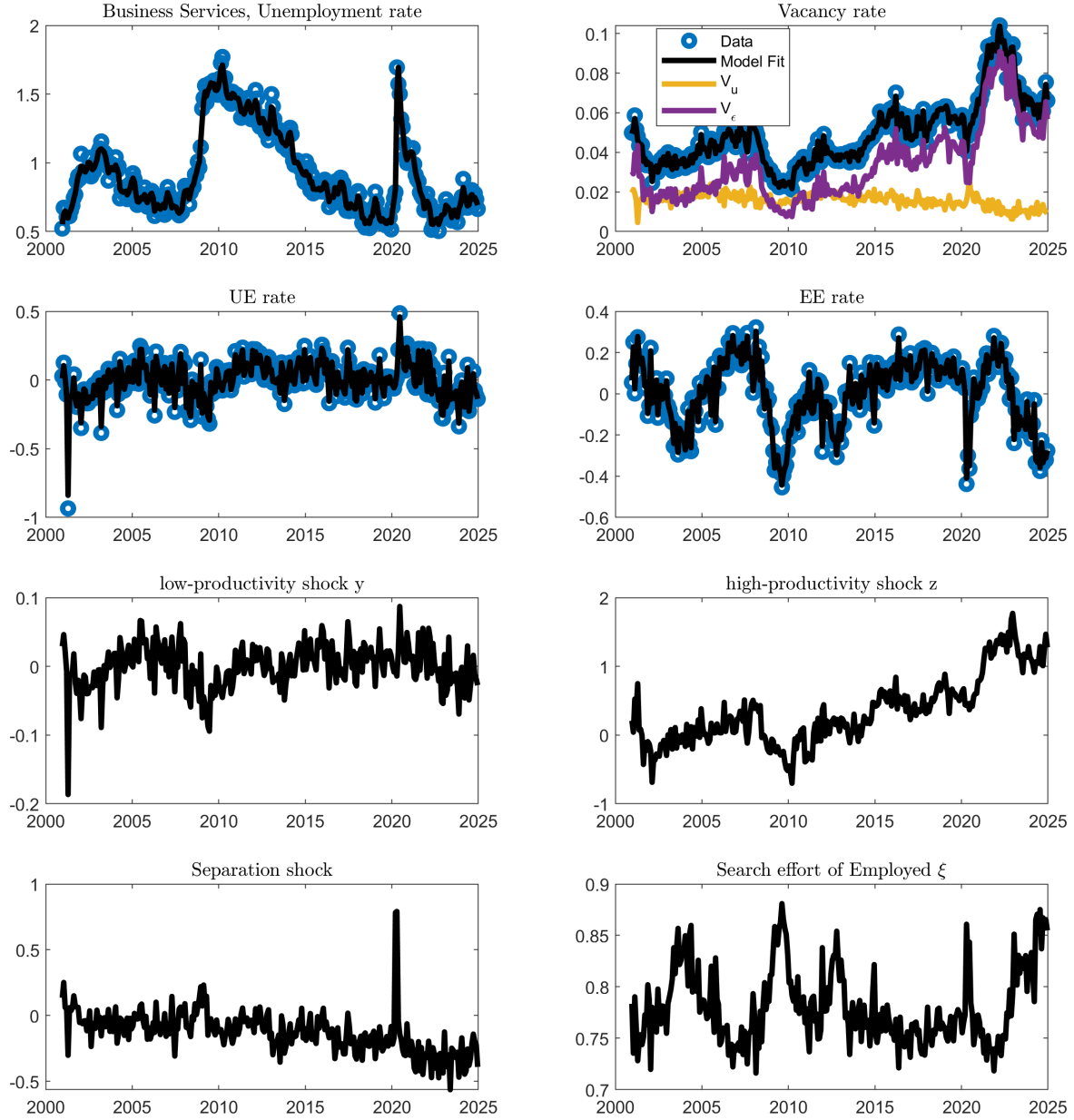


Figure 16: Model Fit and Shocks for Business Services estimation.

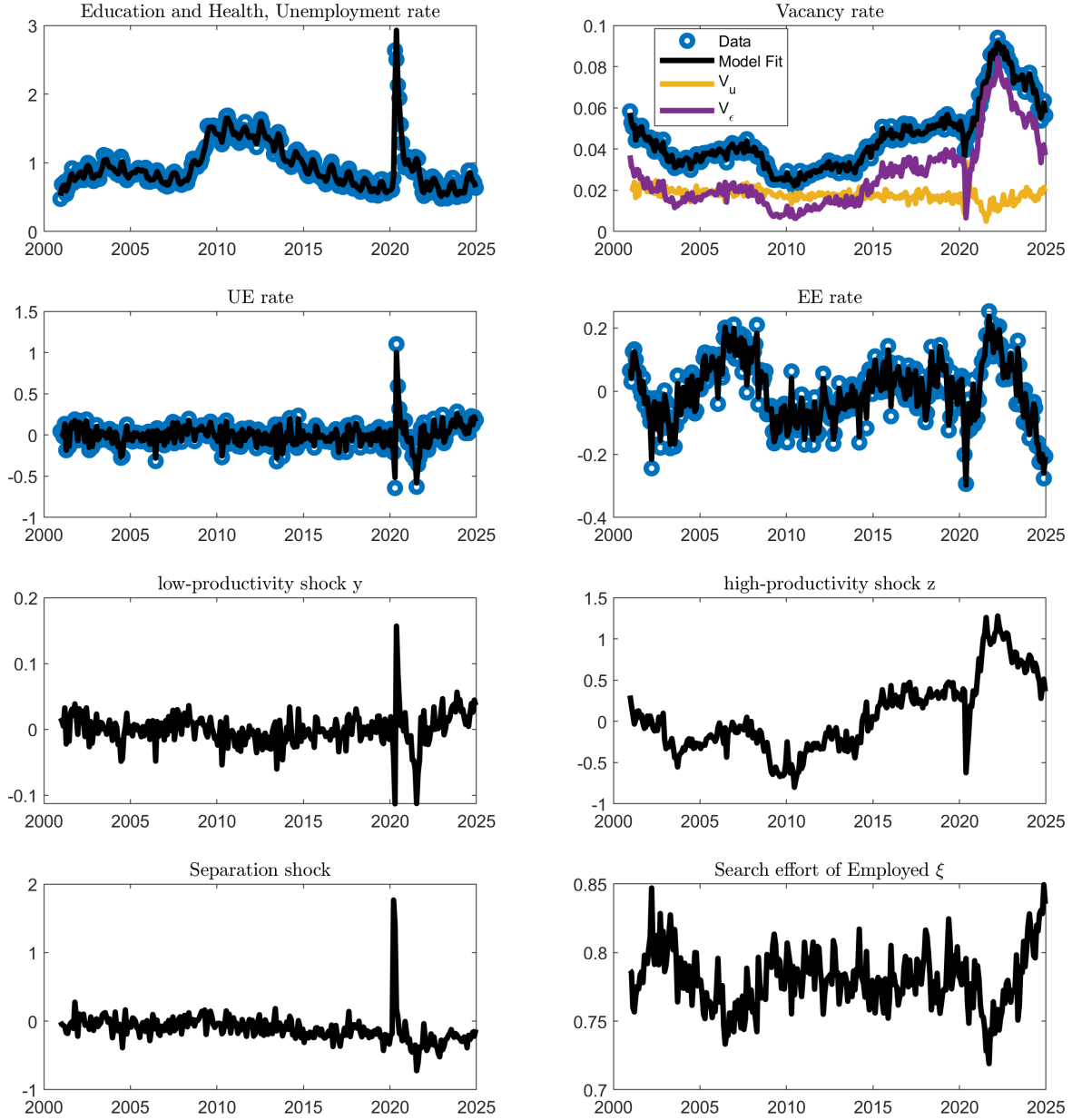


Figure 17: Model Fit and Shocks for Health and Education estimation.